Geofísica Internacional (2017) 56-2: 187-217

Original paper

Shear Wave Splitting and Mantle Flow in Mexico: What Have we Learned?

Raúl W. Valenzuela* and Gerardo León Soto

Received: November 15, 2016; accepted: December 08, 2016; published on line: April 01, 2017

Resumen

El presente artículo es un resumen y análisis de los estudios de partición de ondas transversales (shear wave splitting) para el manto superior que se han realizado en México durante la última década. Cuando una onda sísmica entra en un medio anisótropo se parte (o se separa), esto quiere decir que se producen una onda rápida y otra lenta. Se necesitan dos parámetros para cuantificar la anisotropía. Dichos parámetros son la dirección de polarización rápida y el tiempo de retardo entre la onda rápida y la lenta. Se presenta un ejemplo de la aplicación de la técnica empleando la fase *SKS* ya que la mayoría de las observaciones usan datos telesísmicos. Sin embargo, también se incluyen los resultados de dos estudios que usaron ondas *S* locales de sismos intraplaca. Se explican aspectos importantes para interpretar las mediciones de partición. Entre ellos se incluyen la ubicación de la anisotropía en función de la profundidad, la relación entre la estructura cristalina de la olivina y el flujo del manto, el papel que juega el movimiento absoluto de placas y el papel que juegan los movimientos relativos de placas con un énfasis en las zonas de subducción. Una justificación importante para el estudio de la anisotropía sísmica es que permite conocer las características del flujo en el manto superior así como su relación con procesos tectónicos. México tiene muchos y diversos ambientes tectónicos. Algunos de ellos se encuentran actualmente activos y otros lo fueron en el pasado, pero en cualquier caso han dejado su marca en la forma de anisotropía sísmica. Esto ha dado lugar a una gran variedad de mecanismos para producir el flujo del manto. De manera general la presentación se ha organizado en las siguientes regiones: península de Baja California, la región Mexicana Occidental de Cuencas y Sierras, el norte y noreste de México, la Fosa Mesoamericana, la península de Yucatán y la anisotropía en la base del manto. La relación entre la anisotropía y el flujo del manto se analiza con base en las características particulares de cada región.

Palabras clave: partición de ondas *S,* anisotropía del manto superior, flujo del manto, movimientos de placas, Fosa Mesoamericana, placas de Cocos, Rivera, Pacífico y América del Norte.

R. W. Valenzuela*
Departamento de Sismología
Instituto de Geofísica
Universidad Nacional Autónoma de México
Ciudad Universitaria
Delegación Coyoacán, 04510
Mexico CDMX, México
**Corresponding author: raul@geofisica.unam.mx*

G. León Soto
Instituto de Investigaciones en Ciencias de la Tierra
Universidad Michoacana de San Nicolás de Hidalgo
Morelia, Mich., Mexico

Abstract

A review is presented of the shear wave splitting studies of the upper mantle carried out in Mexico during the last decade. When a seismic wave enters an anisotropic medium it splits, which means that a fast and a slow wave are produced. Two parameters are used to quantify anisotropy. These are the fast polarization direction and the delay time between the fast and the slow wave. An example of the measurement technique is presented using an *SKS* phase because most observations are based on teleseismic data. Results of two studies using local *S* waves from intraslab earthquakes are also discussed. Key aspects of the interpretation of splitting measurements are explained. These include the depth localization of anisotropy, the relationship between olivine fabrics and mantle flow, the role of absolute plate motion, and the role of relative plate motions with a special focus on subduction zones. An important motivation for studying seismic anisotropy is that it makes it possible to constrain the characteristics of upper mantle flow and its relationship to tectonic processes. Mexico has many diverse tectonic environments, some of which are currently active, or were formerly active, and have left their imprint on seismic anisotropy. This has resulted in a wide variety of mechanisms for driving mantle flow. Broadly speaking, the discussion is organized into the following regions: Baja California peninsula, Western Mexican Basin and Range, northern and northeastern Mexico, the Middle America Trench, the Yucatán peninsula, and lowermost mantle anisotropy. Depending on the unique characteristics encountered within each region, the relationship between anisotropy and mantle flow is explored..

Key words: shear wave splitting, upper mantle anisotropy, mantle flow, plate motions, Middle America Trench, Cocos, Rivera, Pacific, and North American plates.

Introduction

Seismic anisotropy is a process whereby elastic waves travel faster in a preferred direction and slower in other directions. It occurs for both *P* and *S* waves, e. g. Savage (1999) and Park and Levin (2002). Different seismic phases, analyzed with different methods, can be used to measure anisotropy. These include studies relying on the refracted *Pn* phase, tomography of both body and surface waves, shear wave splitting, surface wave scattering, and the receiver function technique; see Park and Levin (2002) and Long (2013) for a review. It is the purpose of this paper to focus on shear wave splitting and its relationship to upper mantle flow in Mexico.

When a shear wave propagates through an anisotropic medium, its component polarized parallel to the fast direction gets ahead of its orthogonal component, which is thus known as the slow wave. In this case the fast wave "splits" from the slow one. This phenomenon is the equivalent of the birefringence observed for light (electromagnetic) waves traveling at different speeds within a calcite crystal, as described in optics textbooks, e. g. Hecht (1987). Two parameters are needed to quantify shear wave splitting. These are the polarization direction of the fast wave, ϕ, an angle usually measured clockwise from north, and the delay time, δt, between the fast and the slow wave, e. g. Silver and Chan (1991). Olivine is a major component of the upper mantle and it is an anisotropic mineral (Stein and Wysession, 2003). Mantle anisotropy is the result of the strain induced lattice preferred orientation (LPO) of upper mantle minerals, predominantly olivine (Silver and Chan, 1991; Savage, 1999). As explained below, seismic anisotropy can oftentimes be used to tell the direction of mantle flow and can also be related to different tectonic processes.

Worldwide, shear wave splitting studies of the upper mantle, using teleseismic phases, were published starting in the 1980s once broadband seismometers became widely available (e. g. Ando and Ishikawa, 1982; Ando *et al.,* 1983; Ando, 1984; Kind *et al.,* 1985; Bowman and Ando, 1987; Silver and Chan, 1988, 1991; Vinnik *et al.,* 1989a, 1989b, 1992; Vinnik and Kind, 1993). The methods, as well as the results, have been extensively discussed in several excellent reviews (Silver, 1996; Savage, 1999; Park and Levin, 2002; Long and Silver, 2009a; Long and Becker, 2010). Given that subduction zones play a dominant role as drivers of plate tectonics, their anisotropy structure has been extensively studied (e. g. Long and Silver, 2008, 2009b; Long, 2013; Long and Wirth, 2013; Lynner and Long, 2014a, 2014b; Paczkowski *et al.,* 2014a, 2014b). Shear wave splitting results have been compiled in excellent databases by Liu (2009) for North America, and by Wüstefeld *et al.* (2009) worldwide.

Many studies in Mexico have used teleseismic, core-transmitted phases such as *SKS.* In the earliest work, Barruol and Hoffmann (1999) made a few measurements of shear wave splitting parameters at UNM, the only Geoscope station in Mexico. Later on, van Benthem (2005) made an attempt to present a unified view of upper mantle anisotropy and flow for the entire country, but only a handful of stations were available then. He used data from the permanent network operated by Mexico's Servicio Sismológico Nacional, SSN (Singh *et al.,* 1997), and from the temporary NARS-Baja California deployment (Trampert *et al.,* 2003; Clayton *et al.,* 2004). Later studies were focused, for the most part, on particular regions of the country, using data mostly from temporary arrays. Research in northwestern Mexico (Obrebski *et al.,* 2006; Obrebski, 2007; van Benthem *et al.,* 2008; Long, 2010) used data from the permanent networks Red Sísmica del Noroeste de México, RESNOM (Grupo RESNOM, 2002), and Red Sísmica de Banda Ancha del Golfo de California, RESBAN (Castro *et al.,* 2011), in addition to the temporary NARS-Baja California deployment (Trampert *et al.,* 2003; Clayton *et al.,* 2004). A number of dense, temporary arrays have been used to study subduction of the oceanic Cocos (MASE, 2007; Pérez-Campos *et al.,* 2008; VEOX, 2010; Melgar and Pérez-Campos, 2011; Kim *et al.,* 2011) and Rivera (Yang *et al.,* 2009) plates beneath the continental North American plate. The data from these experiments have been used subsequently to make upper mantle shear wave splitting measurements (Stubailo and Davis, 2007, 2012a, 2012b, 2015; Bernal-Díaz *et al.,* 2008; León Soto *et al.,* 2009; Rojo-Garibaldi, 2011; Bernal-López, 2015; Stubailo, 2015; Bernal-López *et al.,* 2016) and have been helpful to constrain the subslab mantle flow. Additionally, Lynner and Long (2014a) carried out source-side splitting measurements of subslab anisotropy using teleseismic *S* waves after accounting for anisotropy beneath the stations. León Soto and Valenzuela (2013) used *S* phases from local, intraslab earthquakes deeper than 50 km recorded by the VEOX experiment in order to measure anisotropy in the mantle wedge. Recent work has quantified anisotropy using *SKS* data from new SSN stations (Ponce-Cortés, 2012; van Benthem *et al.,* 2013). It is now over a decade since the first results of shear wave splitting in the upper mantle in Mexico were published. It is the purpose of this paper to present a coherent picture of mantle flow for the country. This is appropriate because of the growth the permanent SSN network has experienced (Valdés-González *et al.,* 2005, 2012). Furthermore, the use of permanent and temporary networks together provides a thorough picture, both geographically and in time. Permanent networks are made up of fewer stations located farther apart, but cover a larger area over a long period of time. On the other hand, temporary networks densely cover a smaller area for a few years.

Measurement of Shear Wave Splitting Parameters

Many shear wave splitting studies of the upper mantle in Mexico (van Benthem, 2005; Obrebski *et al.,* 2006; Obrebski, 2007; Stubailo and Davis, 2007, 2012a, 2012b, 2015; van Benthem *et al.,* 2008, 2013; Bernal-Díaz *et al.,* 2008; León Soto *et al.,* 2009; Long, 2009a, 2010; Rojo-Garibaldi, 2011; Ponce-Cortés, 2012; Stubailo, 2015; Bernal-López, 2015; Bernal-López *et al.,* 2016) have worked with core-transmitted phases such as *SKS, sSKS, SKKS,* and *PKS* because they offer several advantages that will be discussed shortly. Most importantly, in the isotropic case **KS* waves are radially (i. e. *SV*-) polarized and thus should not be observed on the transverse component, making it easier to verify that the measured parameters (ϕ, δt) are reliable. The technique used to quantify splitting, however, is more general and can be applied to shear waves containing both *SV* and *SH* energy from local events (e. g. León Soto *et al.,* 2009; León Soto and Valenzuela, 2013).

As mentioned above, the use of core-transmitted waves provides several advantages. (1) For a **KS* phase, the compressional wave traveling through Earth's liquid outer core (the *K* segment) produces only an upgoing *SV*-polarized wave upon entering the mantle. Consequently, in the isotropic case, the **KS* wave will be recorded on the radial component alone and will not be observed on the transverse. Seismic records showing a **KS* arrival on the transverse component are often an indicator of seismic anisotropy under the station (Figure 1a). (2) Given that *SKS* is a teleseismic arrival, its incidence angle at the station is nearly vertical (~10°). *SKS* is most useful for splitting measurements at epicentral distances between 85° and 110° and can thus be used to study anisotropy in regions of no seismic activity such as continental interiors (Silver and Chan, 1988). (3) Since the width of the first Fresnel zone for **KS* phases is on the order of 100 km (Eakin *et al.,* 2015), they provide good lateral resolution and have been used to tell differences between adjacent tectonic domains (e. g. Silver and Chan, 1988; 1991; Silver and Kaneshima, 1993; Silver, 1996; Sheehan *et al.,* 1997). Most often, the anisotropy measured from *KS phases is interpreted to reside in the upper mantle. Care should be taken, however, because core-transmitted phases lack depth resolution and anisotropy can thus accrue anywhere along the upgoing path through the mantle and crust beneath the station (Silver and Chan, 1991; Silver, 1996; Savage, 1999). This issue will be further discussed below.

The procedure to determine the fast polarization direction and the delay time in shear wave splitting analysis is explained in detail by Silver and Chan (1991). Therefore, in the present work, the covariance method is presented in an abridged manner and it is illustrated through an *SKS* measurement. Figure 1a shows the *SKS* wave on the radial and transverse components. Observation of *SKS* as a small, but clear arrival on the transverse component is a plausible indicator of anisotropy beneath the station. In order to measure the anisotropy parameters (ϕ, δt), a window containing the *SKS* pulse in the north-south and east-west components is cut. Subsequently, the N-S and E-W components are rotated in one degree intervals, with ϕ ranging from -90° to 90°. Additionally, for each trial value of ϕ, one component is time-shifted by a time step Δt relative to the other, and the corresponding elements of the covariance matrix are calculated. The *SKS* wave has a dominant period between 10 and 20 s. Observed values of δt usually range from 0.5 to 2.0 s. In the example of Figure 2, Δt = 0.05 s, corresponding to data recorded at 20 samples per second (sps), while trial values of δt fall between 0 and 8 s. In this example Δt = 0.05 s is considered a useful upper bound. Smaller time steps Δt can be chosen for seismograms recorded at greater sampling rates. Small time delays ($\delta t \approx 0.5$ s) are at the resolution limit for core-transmitted waves (Silver and Chan, 1991). In our experience, however, times delays ~0.4 s have been resolved in records having a good signal-to-noise ratio. Furthermore, station-averaged splitting parameters obtained using the method of Wolfe and Silver (1998) provide increased reliability (see below). In the presence of anisotropy, for a well resolved splitting measurement, the covariance matrix will have two nonzero eigenvalues, λ_1 and λ_2 (Silver and Chan, 1991). While searching through parameter space, and considering that noise is present in the records, one has to look for the combination (ϕ, δt) which will produce the most nearly singular covariance matrix (Silver and Chan, 1991). This is usually accomplished by finding the minimum of λ_2, i. e. λ_2^{min} (Figure 2), as in Silver and Chan (1988, 1991). In this plot, the eigenvalues λ_2 obtained for all combinations of ϕ and δt are normalized by dividing by λ_2^{min}. The location of λ_2^{min} is represented by the dot at (74°, 0.95 s).

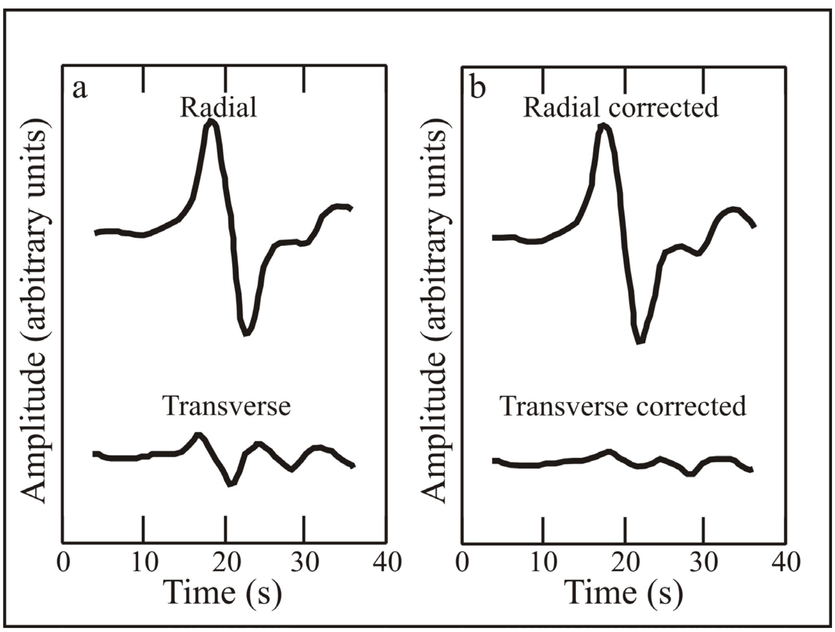

Figure 1. *SKS* wave from the April 8, 1999 event in the Japan Subduction Zone (43.60° N, 130.53° E, h=560 km, M_w = 7.2) recorded at SSN broadband station Mazatlán (MAIG). The epicentral distance is 95.37°. (a) The radial and transverse components are shown. (b) The radial and transverse components are shown after correcting for splitting using the values that were measured. Figure from van Benthem *et al.* (2008).

Other eigenvalue-based measures of linearity such as maximizing λ_1, or λ_1/λ_2, or minimizing $\lambda_1\lambda_2$, have been used by various authors, but these are all equivalent (Silver and Chan, 1991). Finding λ_2^{min} is useful to evaluate the uncertainty of the measured parameters (ϕ, δt) by applying Eq. (16) of Silver and Chan (1991). The first contour around the dot in Figure 2 defines the 95% confidence region for the measurement. In the method of Wolfe and Silver (1998), the contour plots of each individual measurement (earthquake) made at a given station are stacked in order to obtain a robust average measurement for the station having a smaller confidence region. In our experience, small time delays ($\delta t \approx 0.5$ s) are often associated with a large uncertainty in the fast polarization direction. In these cases the stacking method (Wolfe and Silver, 1998) produces well constrained station averages.

Several checks are needed to make sure that the measured splitting parameters are reliable. (1) The N-S and E-W components are rotated and time-shifted by the observed (ϕ, δt) into the fast and slow orthogonal components (Figure 3). Visual inspection of the seismograms should show that the fast and slow shear waveforms are similar, and the fast shear wave should arrive earlier by an amount approximately equal to the measured δt. The fast and slow shear waves must be similar because they originate from the same shear wave within the isotropic medium. Essentially, the covariance method works by finding the values (ϕ, δt) which result in the largest cross-correlation, i. e. similarity, between the fast and slow waves. (2) In the presence of anisotropy, particle motion is elliptically polarized (Figure 4a). Applying a correction to the original components in the amount of (ϕ,

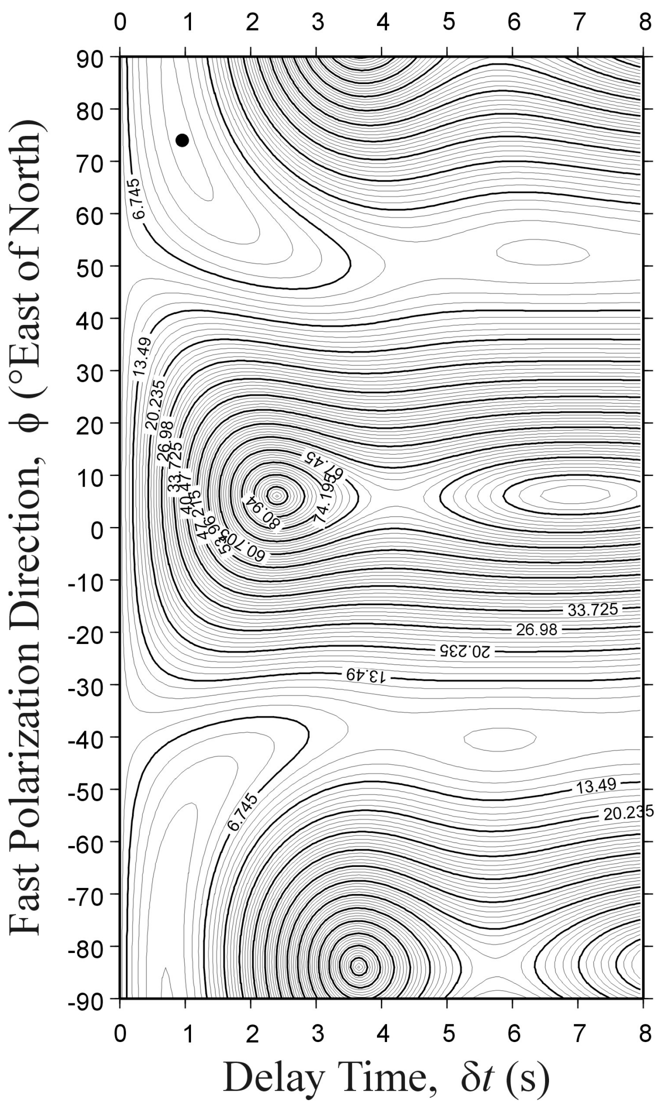

Figure 2. Contour plot showing the minimum value in (ϕ, δt)-space as indicated by the dot. In this case the fast polarization direction is N74°E and the delay time is 0.95 s. The first contour around the dot bounds the 95% confidence region. Figure from van Benthem *et al.* (2008).

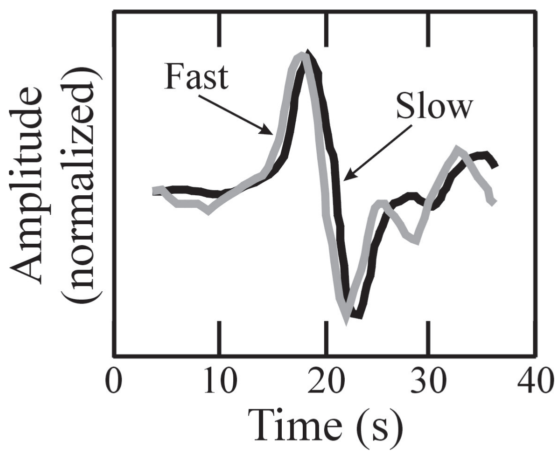

Figure 3. Once the fast polarization direction is known, the N-S and E-W horizontal records are rotated through the angle ϕ in order to obtain the slow and fast components of the *SKS* pulse. The slow and fast components are shown normalized to the same amplitude. Figure from van Benthem *et al.* (2008).

δt) removes the anisotropy, thus resulting in linear particle motion, as shown in Figure 4b for the radial and transverse components of the *SKS* example. (3) In the special case of **KS* waves, removal of the anisotropy returns the energy from the "uncorrected" transverse **KS* wave to the "corrected" radial **KS* pulse, effectively removing it from the "corrected" transverse component (Figure 1b). The amplitude of the "corrected" radial **KS* pulse is larger than the amplitude of the "uncorrected" radial **KS,* although this effect is too small to notice in Figure 1b.

Variations of the method described above have been used by different authors. In the special case of **KS* core-transmitted phases, the energy on the trial transverse component can be minimized instead of λ_2 (Silver and Chan, 1988, 1991). Additionally, given that **KS* on the transverse component in an isotropic medium is zero, and if the delay time, δt, is small compared to the characteristic period of the wave being used, then the transverse component **KS* within an anisotropic medium is approximately proportional to the time derivative of **KS* on the observed radial component (Silver and Chan, 1988, 1991; Vinnik *et al.,* 1989b). Vinnik *et al.* (1989b) take advantage of this fact and synthesize the trial transverse component **KS* waveform from the observed radial component. The parameters (ϕ, δt) are determined by minimizing the difference between the synthetic and observed transverse **KS* pulse.

Interpreting Shear Wave Splitting Measurements

In order to interpret the results of shear wave splitting measurements, it is necessary to resolve certain issues such as the actual localization of the anisotropy along the path from the core-mantle boundary to the stations, the relationship between simple shear and the direction of mantle flow depending on the various fabrics of olivine, and the relationship between tectonic processes and the anisotropy they cause. These topics are discussed in the present section.

Depth Localization of Anisotropy

Given that for **KS* phases anisotropy accrues all along the upgoing path through the mantle and crust beneath the station (Silver and Chan, 1991; Silver, 1996; Savage, 1999), it is important to determine where the main contribution to anisotropy is localized. Careful studies using stations that have data sampling from many different back azimuths, as well as comparison of splitting parameters measured from similar back azimuths at nearby stations

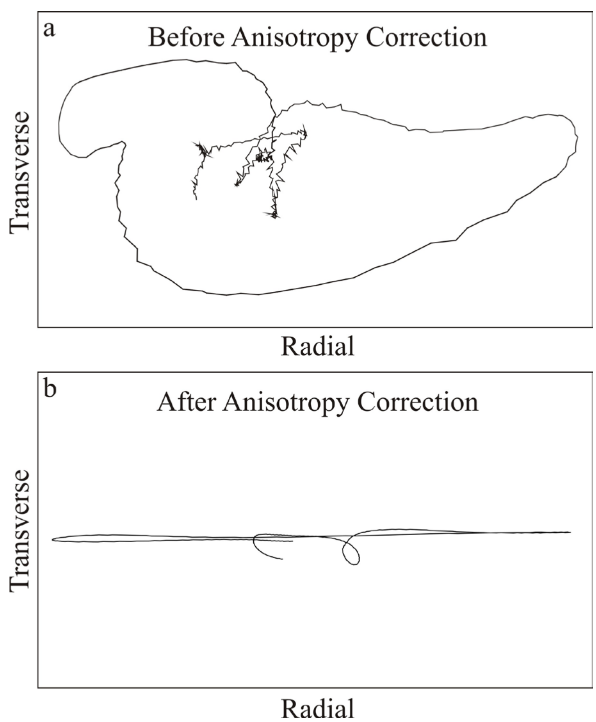

Figure 4. A further check is the comparison of the radial and transverse particle motion. (a) Before correcting for the anisotropy the particle motion is elliptical. (b) Once a correction for the measured anisotropy is applied, the particle motion becomes nearly linear. Figure from van Benthem *et al.* (2008).

(Ando *et al.,* 1983; Silver and Chan, 1988; Savage and Silver, 1993; Gao *et al.,* 1994; Alsina and Snieder, 1995; Hirn *et al.,* 1995; Guilbert *et al.,* 1996; Sheehan *et al.,* 1997; Savage, 1999), concluded that in many cases most of the observed anisotropy is found in the upper mantle, with little to no splitting below 400-600 km depth (Vinnik *et al.,* 1992, 1995, 1996; Barruol and Mainprice, 1993; Mainprice and Silver, 1993; Savage, 1999). In fact, most shear wave splitting studies base their interpretations on tectonic processes occurring in the upper mantle. In some regions, however, evidence has emerged for anisotropy in the lowermost upper mantle and in the uppermost lower mantle (Wookey *et al.,* 2002; Chen and Brudzinski, 2003; Wookey and Kendall, 2004; Foley and Long, 2011; Di Leo *et al.,* 2012; Kaneshima, 2014; Lynner and Long, 2014a), as well as in the D" layer at the base of the mantle (Long, 2009a). Additionally, the contribution from the crust must also be assessed. Shear wave splitting measurements of crustal anisotropy around the world have obtained delay times ranging mostly from 0.1 to 0.3 s, and averaging to 0.2 s (Kaneshima, 1990; Silver and Chan, 1991; Silver, 1996; Crampin and Gao, 2006). Several causes for crustal anisotropy have been proposed (e. g. Balfour *et al.,* 2005, 2012). One common explanation suggests that fluid-filled cracks align preferentially in the direction of maximum compressive stress (Crampin, 1994; Balfour *et al.,* 2005, 2012) and are located in the top 10 to 15 km of the crust (Kaneshima *et al.,* 1988; Kaneshima, 1990; Crampin, 1994; Silver, 1996). Mineral alignment associated with foliation in schist or shearing in fault zones is another possible source of anisotropy (Balfour *et al.,* 2005, 2012; Boness and Zoback, 2006). It has been suggested that in the upper crystalline crust, anisotropy may be due to cracks and produced as a result of stress, whereas in the lower crust it may be caused by mineral alignment from sheared and metamorphosed rocks (Babuska and Cara, 1991; Savage, 1999; Balfour *et al.,* 2012). If two or more anisotropic layers are present under a station, and if the fast axes of these layers are not oriented in the same direction, then it is not possible to calculate a simple, arithmetic sum of the delay times in each layer. The measured, apparent splitting parameters (ϕ_a, δt_a) can be expressed as trigonometric functions of the splitting parameters of the individual layers (ϕ_1, δt_1) and (ϕ_2, δt_2); see Savage and Silver (1993), Silver and Savage (1994), and Özalaybey and Savage (1994, 1995). Typical delay times determined from **KS* phases are on the order of 1 s, which is about five times the average crustal delay time of 0.2 s (Silver, 1996). To summarize, the crustal contribution to **KS* splitting is small, and it is generally agreed that the main contribution to the splitting parameters comes from the uppermost mantle (Silver, 1996). Furthermore, in order that the physical mechanisms explained below can give rise to anisotropy, it is necessary that anisotropy be localized in the upper mantle.

Olivine Fabrics and Mantle Flow

Observations of upper mantle xenoliths (Christensen, 1984; Nicolas and Christensen, 1987; Mainprice and Silver, 1993), together with laboratory experiments (Zhang and Karato, 1995; Jung *et al.,* 2006), have established that when flow occurs in simple shear, the *a* axis of olivine, and consequently the fast polarization direction, ϕ, becomes oriented in the direction of mantle flow (Silver, 1996; Savage, 1999; Jung *et al.,* 2006; Wiens *et al.,* 2008). The olivine fabric described in the preceding studies eventually became known as A-type. Experimental results have shown that A-type LPO fabric develops under relatively low stresses, high temperature, and low water content (Karato *et al.,* 2008). Therefore, it has traditionally been accepted that A-type olivine prevails under the continental and oceanic crust (Karato *et al.,* 2008), and it is also expected in the mantle wedge core (Kneller *et al.,* 2005; Jung *et al.,* 2006; Long and Silver, 2008). Subsequently, Jung and Karato (2001) reported on the existence of B-type fabric and showed that in this case the fast polarization direction, ϕ, is perpendicular to the direction of mantle flow. B-type olivine develops under low temperature, high water content, and high stress conditions and is often present in the mantle wedge tip (Kneller *et al.,* 2005; Jung *et al.,* 2006; Long, 2013). Later work has continued down the alphabet and has characterized C-, D- and E-type olivine (e. g., Jung and Karato, 2001; Kneller *et al.,* 2005; Jung *et al.,* 2006; Karato *et al.,* 2008). For instance, B-, C- and E-types exist under moderate to high water content conditions (Kneller *et al.,* 2005; Jung *et al.,* 2006). For the purposes of the present review, it suffices to say that C-, D-, and E-type fabrics all show seismic fast axes oriented in the direction of mantle flow (Jung *et al.,* 2006; Long, 2009b), and are thus similar to A-type olivine in this regard.

Relation of Splitting to Tectonic Processes

One important aspect of interpreting shear wave splitting measurements concerns the relationship they hold with various tectonic processes. These can be generally divided into processes affecting sites in the stable continental interior and sites located at plate boundaries. Of the latter, subduction zones have received special attention. These relationships are explored below.

Absolute Plate Motion

Under this hypothesis, the hot spot reference frame absolute plate motion (APM) of the rigid lithosphere drags the asthenosphere underneath, driving mantle flow in the same direction as APM (Silver, 1996). This effect is strongest at the lithosphere-asthenosphere boundary and decreases with increasing depth. In this view, the asthenosphere is a shear zone that concentrates strain, decouples the lithosphere from the slowly moving mantle below and produces anisotropy (Silver, 1996). This hypothesis is also known as simple asthenospheric flow, SAF, (Silver, 1996) and predicts that observed fast polarization directions are aligned with the direction of APM. It is frequently accepted that anisotropy produced by APM is the result of an active, ongoing process (Silver, 1996). In the absence of "fossil", lithospheric anisotropy from earlier tectonic events (see below), splitting measurements in the stable plate interiors are best explained by the APM hypothesis. Predictions from SAF work reasonably well for sites in fast-moving plates such as North America (Silver and Chan, 1991), although local tectonic effects can also be important. Several experiments in the United States have shown that North American APM explains the fast axes in the stable continental interior (e. g. Fouch *et al.,* 2000; Refayee *et al.,* 2014; Hongsresawat *et al.,* 2015).

Relative Plate Motion

This hypothesis is most relevant at plate boundaries, whether they be current or ancient. It posits that tectonic processes acting at plate boundaries cause deformation of the crust which extends into the lithospheric mantle and it is also called vertically coherent deformation, or VCD (Silver and Chan, 1988, 1991; Silver, 1996). Three different types of plate boundaries exist, and these are: transcurrent, convergent, and divergent (e. g. Levin, 1986). The expected alignment of the seismic fast polarization directions depends on the type of plate boundary as follows. For strike-slip, or transcurrent, boundaries, the seismic fast polarization direction is expected to align parallel to the transcurrent structure (Silver, 1996; Savage, 1999). Collisional structures often involve oblique convergence with a significant transcurrent component in a process referred to as transpression (Vauchez and Nicolas, 1991; Silver, 1996; Savage, 1999). Therefore, a component of mantle flow occurs parallel to the strike of transpressional structures, thus leading to strike-parallel seismic fast axes (Nicolas, 1993; Silver, 1996; Savage, 1999). For divergent boundaries the fast axis should become parallel to the extension direction outside the ridge (Silver, 1996; Blackman and Kendall, 1997; Savage, 1999), but directly below the ridge it may be parallel to the ridge axis (Blackman and Kendall, 1997; Savage, 1999).

During a tectonic episode, deformation and creation of seismic anisotropy may occur at temperatures in excess of 900°C. Once the lithospheric mantle temperature drops below this threshold, anisotropy may become "fossilized" (Silver and Chan, 1988, 1991; Silver, 1996) or "frozen-in" (Vinnik *et al.,* 1992; Savage, 1999). Barring the occurrence of a more recent tectonic event, fossil or ancient anisotropy may be preserved and can be detected at present. Under stable continental cratons, anisotropy may have remained frozen since the Archean, i. e. between 2.6 and 3.8 Ga (Silver and Chan, 1991; Silver and Kaneshima, 1993; Silver, 1996; Savage, 1999).

Subduction Systems

Subduction zones represent a particular case of convergent boundaries. Oceanic lithosphere originally created at spreading centers is recycled back into the mantle in subduction zones (e. g. Levin, 1986; Stein and Wysession, 2003). Furthermore, the negative buoyancy of subducting slabs is believed to provide the main force driving plate tectonics (Stegman *et al.,* 2006). Additionally, deep earthquakes occurring within some slabs down to depths of 660 km are useful sources to sample mantle anisotropy, both locally and teleseismically (Savage, 1999; Long and Silver, 2009b; Long, 2013). So, seismic anisotropy in subduction zones has come under close scrutiny (e. g. Savage, 1999; Long and Silver, 2008, 2009b; Long, 2013; Long and Wirth, 2013; Lynner and Long, 2014a, 2014b; Paczkowski *et al.,* 2014a, 2014b). Yet, the anisotropic structure of subduction zones is complicated because it is hard to separate the different contributions from the subslab mantle, the slab itself, the mantle wedge, and the overlying plate (Savage, 1999; Long and Silver, 2008). Generally, two different processes are recognized to control upper mantle flow and anisotropy in subduction systems. These are downdip motion of the slab and trench migration (Long and Silver, 2008).

Downdip motion of the slab.- Viscous coupling between the downgoing slab and the surrounding asthenospheric mantle drives mantle flow parallel to the subduction direction (Savage, 1999; Long and Silver, 2008). Within the mantle wedge this is called *corner flow,* whereas beneath the slab it is known as *entrained flow* (Long and Silver, 2008). Under the assumption of A-type (or similar) olivine, seismic fast axes are expected to align in the direction of relative plate motion between the overriding and subducting plates, or roughly trench-perpendicular, both above and below the slab. In this case mantle flow is two-dimensional (2-D). Because of their nearly vertical incidence angles, *SKS* anisotropy measurements are only sensitive to the horizontal component of upper mantle flow.

Trench migration.- Trenches are not stable with respect to a fixed reference frame (Stegman *et al.,* 2006). Slabs move in a downdip slab-parallel direction and also in a slab-perpendicular direction (Schellart, 2004), either backward (trench retreat or slab rollback) or forward (trench advance). Slabs do not have an infinite width in the trench-parallel direction. Instead, their width is finite and ranges between 200 and 5000 km (Stegman *et al.,* 2006). Consequently, trench migration induces toroidal flow around the lateral edges of the slab within a roughly horizontal plane (Schellart, 2004; Stegman *et al.,* 2006). Slab rollback drives 3-D *return flow* of the mantle from beneath the slab, around the slab edge, and into the mantle wedge (Schellart, 2004; Stegman *et al.,* 2006). It has been further proposed that a barrier, probably at the top or the bottom of the transition zone, keeps mantle from flowing under the slab tip (Russo and Silver, 1994; Savage, 1999; Schellart, 2004; Long and Silver, 2008, 2009b). Such a barrier could be due to the increased viscosity at the upper-lower mantle boundary, or to the high pressure beneath the slab produced by the sinking slab (Schellart, 2004). It has been suggested that this barrier causes trench-parallel mantle flow, both beneath the slab (Russo and Silver, 1994; Long and Silver, 2008, 2009b) and in the mantle wedge fore-arc (Long and Silver, 2008). Additionally, a mechanism is needed to decouple the subslab mantle from the slab itself so that flow does not become entrained. It has been proposed that the asthenosphere which is in contact with the bottom of the slab experiences a large amount of shear strain, forming a thin layer which becomes entrained and which acts as a weak decoupling zone (Phipps Morgan *et al.,* 2007; Long and Silver, 2008, 2009b). This thin asthenospheric layer is subjected to shear heating during deformation, and is therefore hot and buoyant as a result of increased temperature and reduced viscosity (Long and Silver, 2009b). Since LPO is of A-type (or similar), trench-parallel flow produces trench-parallel fast polarization directions in the subslab mantle (Long and Silver, 2008, 2009b). Within the mantle wedge fore-arc, trench-parallel flow is hypothesized to lead to high mantle flow velocities, which in turn removes cool wedge material (Long and Silver, 2008). The resulting high temperatures are compatible with A-type (or similar) LPO and with trench-parallel fast axes (Long and Silver, 2008).

Thorough reviews have shown that trench-parallel fast axes are predominant in the subslab mantle and it has been suggested that trench migration is the main agent driving trench-parallel mantle flow in subduction systems (Long and Silver, 2008, 2009b; Long, 2013). The Cascadia, Greek, and Mexican subduction zones represent exceptions where mantle flow is entrained beneath the slab, producing trench-perpendicular fast polarization directions (Long and Silver, 2008, 2009b; Long, 2013). Most of the previous studies were based on *SKS* measurements of seismic anisotropy, with appropriate corrections from local events in the mantle wedge where available (Long and Silver, 2008, 2009b). Recent work obtained source-side measurements of subslab anisotropy using intraslab sources after making the appropriate corrections for anisotropy under the receiver (Lynner and Long, 2013, 2014a, 2014b). These studies found additional subduction zones with trench-perpendicular fast axes in Central America, Alaska-Aleutians, Ryukyu, western Sumatra, and northern Kurils (Lynner and Long, 2014a). Thus, Lynner and Long (2014a) concluded that subslab seismic fast axes are more common than previously believed (Long and Silver, 2008, 2009b).

Several mechanisms have been proposed to account for the differences between subduction zones where subslab fast axes are trench-parallel and those with trench-perpendicular observations. A thorough discussion of these models is outside the scope of the present review, but they will be listed. The reader is referred to the original articles, or alternatively, to the summary by Bernal-López *et al.* (2016). The first mechanism is shear heating (Long and Silver, 2008, 2009b) as described above. Song and Kawakatsu (2012) proposed that the oceanic asthenosphere has orthorhombic anisotropy, and that the dip of the slab controls the orientation of the seismic fast axes. Numerical modeling by Paczkowski et al. (2014a, 2014b) found that long and steep slabs are consistent with trench-parallel fast axes, whereas short slabs which do not penetrate into the lower mantle should produce trench-perpendicular fast polarization directions. Lastly, Lynner and Long (2014a, 2014b) suggested that differences in slab age, with a dividing line around 95 Ma, produce different lithospheric structures, such that trench-perpendicular fast axes are associated with younger lithosphere and trench-parallel fast polarization directions are correlated with older lithosphere.

Shear Wave Splitting Observations in Mexico

Figure 5a shows the averaged splitting parameters calculated from individual **KS* measurements made at each station of the permanent SSN, RESNOM, and RESBAN, and the temporary NARS-Baja California networks. The densest coverage is found in tectonically and seismically active regions. These are the transform-extensional boundary between the North America and Pacific plates in the Gulf of California (northwestern Mexico), and subduction of the Rivera and Cocos plates under the North America and Caribbean plates at the Middle America Trench (MAT) in southern Mexico. A few SSN stations are located in northern and northeastern Mexico, and in the Yucatán peninsula in easternmost Mexico. The ensuing discussion is organized around the various tectonic regions. Figure 5b shows the locations of various geographic features in Mexico discussed in the text.

Baja California Peninsula

Station-averaged shear wave splitting measurements for the Baja California Peninsula (van Benthem, 2005; Obrebski *et al.,* 2006; Obrebski, 2007; van Benthem *et al.,* 2008; Liu, 2009; Ponce-Cortés, 2012) are summarized in Figure 6. Results can be organized into three different regions based on the observed splitting parameters and also on the geologic and tectonic history. These regions are the northern peninsula, the southern peninsula, and one single measurement at the southernmost tip of the peninsula. Furthermore, observed shear wave splitting fast axes are consistent with those obtained from Rayleigh wave tomography at periods from 80 to 100 s along the entire length of the peninsula (Zhang *et al.,* 2007, 2009; van Benthem *et al.,* 2008). Interestingly, the velocity structure determined from surface waves is also consistent with these three different regions. At periods from 50 to 80 s, slow velocities are observed under the northern peninsula and at its southenmost tip, whereas fast velocities are obtained in between (Zhang *et al.,* 2007, 2009). Zhang *et al.* (2007) interpreted the high velocities in the southern half of the peninsula as the remnants of the stalled Magdalena and Guadalupe microplates, and associated the slow velocities under the northern half to the slab window created during subduction of the Farallon plate. The splitting fast axes in the northern peninsula are generally oriented E-W and have delay times ranging from 0.70 to 2.20 s (Obrebski *et al.,* 2006; Obrebski, 2007); see Figure 6. These observations are consistent with shear wave splitting measurements across the international boundary in California (Savage and Silver, 1993; Özalaybey and Savage, 1995; Polet and Kanamori, 2002; Hongsresawat *et al.,* 2015). Savage and Silver (1993) and Özalaybey and Savage (1995) observed a pattern of E-W fast axes in California between the southern end of the subducting Gorda plate and as far south as the southern end of the state, and also in western Nevada. They explained this pattern by mantle upwelling and subsequent horizontal flow which fills the slabless window left by the subducted Farallon plate. For southwestern California, Silver and Holt (2002) proposed that differential motion between the North American plate and sinking fragments of the Farallon plate control asthenospheric flow. Obrebski *et al.* (2006) thus proposed asthenospheric flow induced by a sinking fragment of the Farallon plate as their preferred mechanism to explain the anisotropy observed under northern Baja California. Alternatively, Bohannon and Parsons (1995) suggested that a fragment of the Farallon plate may have been captured east of the former trench. Magnetotelluric measurements by Romo *et al.* (2001) are consistent with the existence of a captured fragment. Therefore, fossil anisotropy in a captured fragment of the Farallon plate is also a possible explanation for the observed anisotropy (Obrebski *et al.,* 2006).

Shear wave splitting observations in the southern half of the Baja California peninsula are indicative of little to no anisotropy (van Benthem *et al.,* 2008); see Figure 6. Several stations have short delay times between 0.50 and 0.75 s, whereas other stations produce null measurements which can be interpreted either as the absence of detectable anisotropy ($\delta t <$ 0.5 s) or the lack of data with the proper back azimuth to return a split measurement (Figure 6). The young Guadalupe and Magdalena microplates subducted under southern Baja California (Bohannon and Parsons, 1995). Subduction of the Magdalena microplate

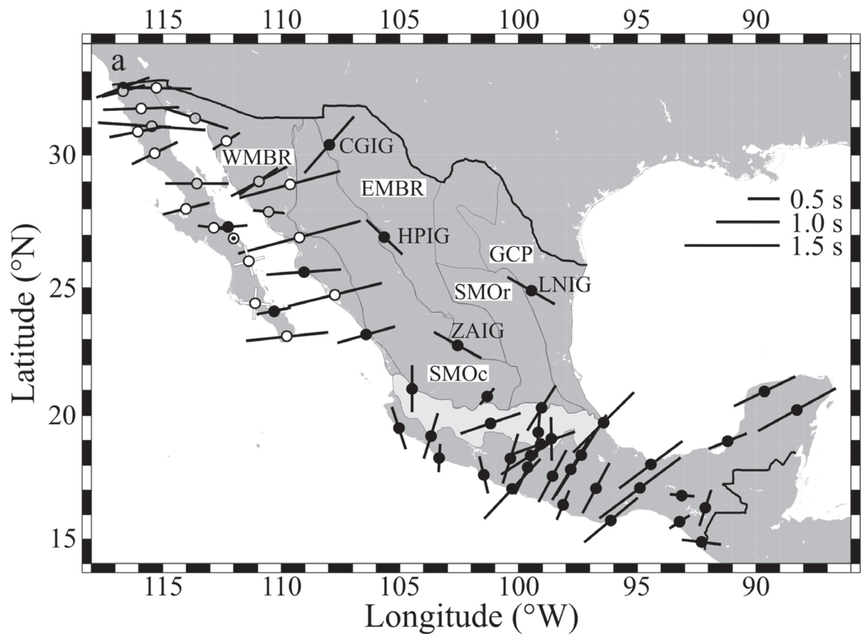

Figure 5a. Station-averaged splitting parameters in Mexico. The length of the bars is proportional to δt, as indicated in the legend. Black dots represent SSN stations (van Benthem, 2005; van Benthem *et al.,* 2008, 2013; Ponce-Cortés, 2012), gray dots are for RESNOM and RESBAN stations (Obrebski *et al.,* 2006; Obrebski, 2007), and white dots stand for the NARS-Baja California deployment (van Benthem, 2005; Obrebski *et al.,* 2006; Obrebski, 2007; van Benthem *et al.,* 2008; Liu, 2009). Thick black lines represent the international borders; with the United States to the north, and with Guatemala and Belize to the south. The TMVB is indicated by light shading. Tectonic provinces of northern Mexico are labeled: Western Mexican Basin and Range (WMBR), Sierra Madre Occidental (SMOc), Eastern Mexican Basin and Range (EMBR), Sierra Madre Oriental (SMOr), and Gulf Coastal Plain (GCP). Tectonic provinces after Ortega-Gutiérrez *et al.* (1992).

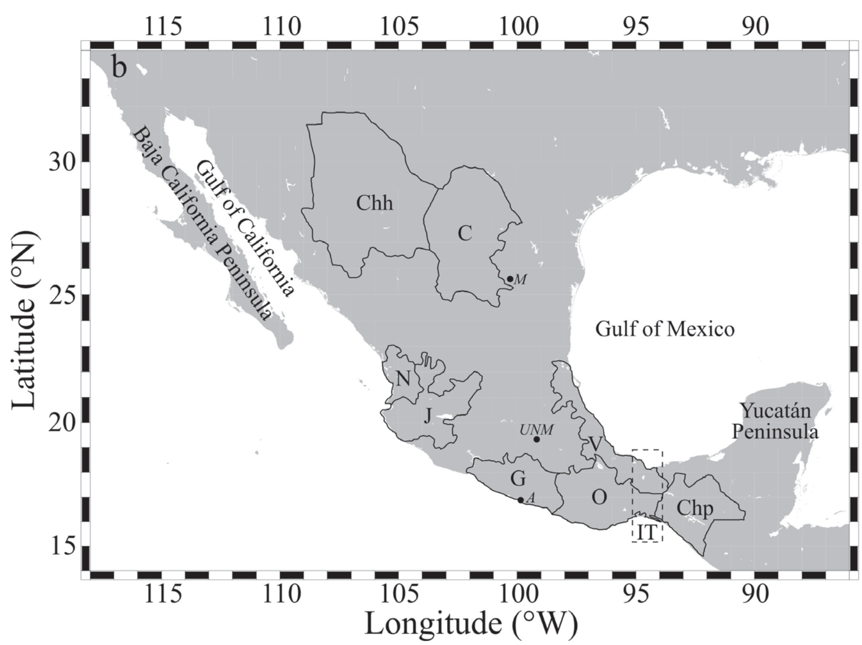

Figure 5b. Map showing geographic features in Mexico discussed in the text. Outlines represent Mexican states: Chihuahua (Chh), Coahuila (C), Nayarit (N), Jalisco (J), Veracruz (V), Guerrero (G), Oaxaca (O), and Chiapas (Chp). Dots are cities: Monterrey (*M*) and Acapulco (*A*). Location of seismic station *UNM* in Mexico City is shown. IT stands for Isthmus of Tehuantepec.

produced arc magmatism between 24 and 12.5 Ma (Sedlock *et al.,* 1993; Sedlock, 2003; Fletcher *et al.,* 2007). By 12.5 Ma, the southern Baja California peninsula was positioned over the thermal anomaly of the former Magdalena ridge, causing asthenospheric upwelling through the broken Magdalena slab (Fletcher *et al.,* 2007). Given that shear wave splitting measurements are only sensitive to horizontal flow, van Benthem *et al.* (2008) proposed vertical upwelling as the explanation for the small delay times observed. A second possibility is that shear wave splitting measurements may be influenced by fossil anisotropy (or rather, the absence of anisotropy) in the remants of the stalled Magdalena and Guadalupe microplates (van Benthem *et al.,* 2008).

A single station in the southernmost tip of the peninsula records an average delay time of 1.30 s and a fast axis oriented roughly E-W, a pattern which is most consistent with anisotropy in the northern half of the peninsula (van Benthem *et al.,* 2008); see Figure 6. In addition to the velocity and anisotropy structures determined from surface waves (Zhang *et al.,* 2007, 2009) as discussed above, the geological units on the peninsula are also consistent with the shear wave splitting observations. In the northern half, and at the southernmost tip, of the peninsula granitic rocks are exposed (Ortega-Gutiérrez *et al.,* 1992). In fact, the souterhnmost granitic unit was continuous with rocks on the mainland in Jalisco and Nayarit states before the peninsula

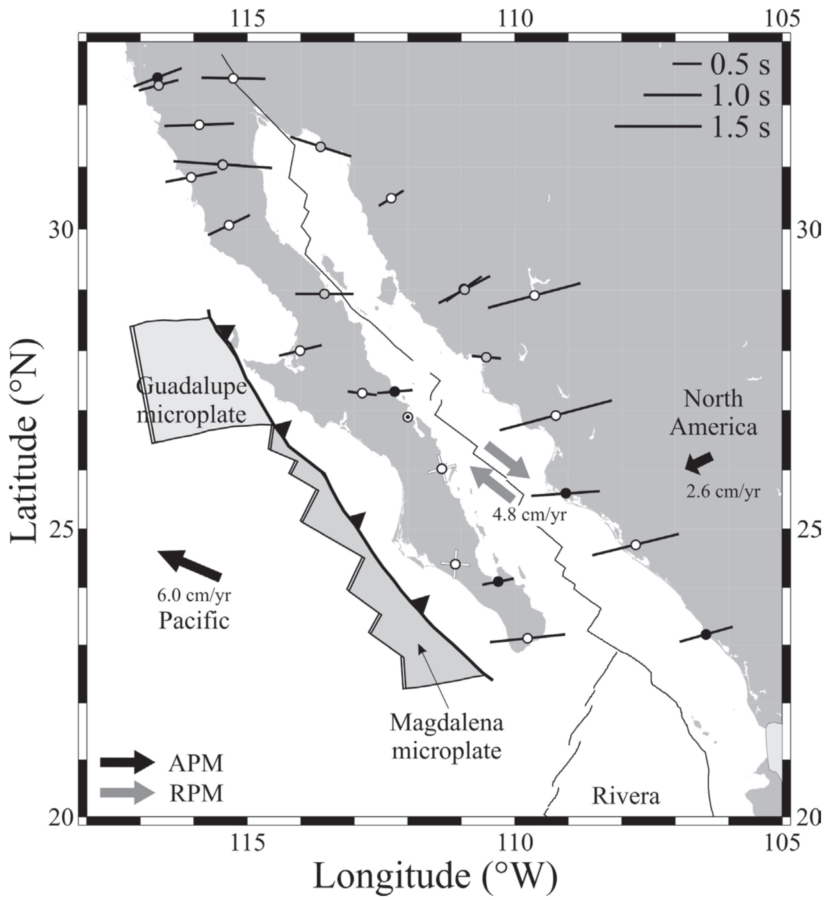

Figure 6. Station-averaged splitting parameters in northwestern Mexico. The length of the bars is proportional to δt, as indicated in the legend. Black dots represent SSN stations (van Benthem, 2005; van Benthem *et al.,* 2008; Ponce-Cortés, 2012), gray dots are for RESNOM and RESBAN stations (Obrebski *et al.,* 2006; Obrebski, 2007), and white dots stand for the NARS-Baja California deployment (van Benthem, 2005; Obrebski *et al.,* 2006; Obrebski, 2007; van Benthem *et al.,* 2008; Liu, 2009). Black arrows indicate the direction of absolute plate motion (APM) of the Pacific and North American plates (Gripp and Gordon, 2002). Gray arrows show the direction of the relative plate motion (RPM) between these two plates (DeMets *et al.,* 1994). Location of Guadalupe and Magdalena microplates relative to the Baja California peninsula at the time subduction stopped (12.3 Ma) from Fletcher *et al.* (2007). Barbed line represents the paleotrench. The Baja California peninsula, and the Guadalupe and Magdalena microplates are currently part of the Pacific plate.

rifted away (Ortega-Gutiérrez *et al.,* 1992). In between the peninsular granitic rocks, in most of the southern peninsula, igneous extrusive rocks associated to subduction of the Magdalena microplate are exposed (Ortega-Gutiérrez *et al.,* 1992; Sedlock *et al.,* 1993; Sedlock, 2003; Fletcher *et al.,* 2007). Therefore, the large delay times and E-W fast axes observed in the northern half and at the southermost tip of the peninsula record the mantle flow pattern produced by subduction of the extinct Farallon plate (van Benthem *et al.,* 2008). In between, in most of the southern half of the peninsula, subduction of the young Guadalupe and Magdalena microplates resulted in a vertical mantle flow pattern and different rock units (van Benthem *et al.,* 2008). While subduction of the Farallon and Magdalena plates occurred simultaneously, Cenozoic, extrusive volcanism only occurred associated to the young Magdalena microplate (Ortega-Gutiérrez *et al.,* 1992). This volcanism is not observed at the southernmost tip of the peninsula, in the Los Cabos and Trinidad blocks, which are distinct from the Comondú volcanics in the rest of the southern Baja California peninsula (Ortega-Gutiérrez *et al.,* 1992; Sedlock *et al.,* 1993; Fletcher *et al.,* 2007).

In addition to the work discussed above (Obrebski *et al.,* 2006; van Benthem *et al.,* 2008, O06 and B08, respectively), **KS* shear wave splitting measurements using NARS-Baja California data were made by Long (2010). While the measurements of O06 and B08 are broadly consistent with those of Long (2010) at many stations, Long (2010) identified discrepancies between the measurements made by O06 and B08 and her own measurements at several stations. Some of these differences may arise as a consequence of the different bandpass filters used. Long (2010) worked at relatively low frequencies, whereas O06 and B08 leaned towards using broader bandpass filters to the extent that the signal-to-noise ratio of the data allowed it. Also, a major focus of the work by Long (2010) was on frequency-dependent shear wave splitting. The complex splitting patterns and observed frequency dependence argue for anisotropic structure that is highly heterogeneous, and both lateral and vertical variations in anisotropy are likely (Long, 2010). While O06 and B08 recognized the complexity of the dataset, their approach was to come up with the simplest possible tectonic interpretation. Furthermore, the measurements made at permanent stations by O06 and B08 are generally supportive of their NARS-Baja California interpretations. Obrebski and Castro (2008) addressed some of the complex anisotropy questions in the crust/lithosphere working with receiver functions at selected stations of the NARS-Baja California array. In spite of the complex tectonic environment and the different filters chosen, however, the results from O06 and B08 are generally consistent with those of Long (2010). For instance, B08 agree with Long (2010) on the existence of a region of weak and/or complex anisotropy in the southern half of the peninsula. Additionally, some E-W fast axes in the northern half of the peninsula are consistent between O06 and Long (2010), and also some ENE-WSW fast axes in the Western Mexican Basin and Range (next subsection) are consistent between B08 and Long (2010). With respect to the interpretation of results, Long (2010) agrees that the Guadalupe microplate plays a role in controlling the weak anisotropy observed in the southern half of the Baja California peninsula. Unlike van Benthem *et al.* (2008), however, she proposed that coherent mantle flow is inhibited by the lodged fragments of the Guadalupe microplate. On the other hand, Wang *et al.* (2009) report on the existence of several buoyant mantle upwellings associated to some of the basins in the Gulf of California. Thus, Long (2010) proposed that the orientation of the fast axes at the three northernmost peninsular stations of the NARS-Baja California deployment is the result of horizontal flow away from the upwelling centered in the Wagner Basin.

Western Mexican Basin and Range

The Western Mexican Basin and Range (WMBR) is an extensional province bounded to the west by the Gulf of California and to the east by the Sierra Madre Occidental, or SMOc (Sedlock *et al.,* 1993). The WMBR is the southern continuation of the well-known Basin and Range province in the southwestern United States (Sedlock *et al.,* 1993). Shear wave splitting measurements in the southern WMBR show fast polarization directions consistently oriented ENE-WSW and large delay times ranging between 0.95 and 2.00 s (Obrebski *et al.,* 2006; van Benthem *et al.,* 2008); see Figure 6. In the northern WMBR delay times are generally less than 1 s and fast axes orientations are somewhat variable (Obrebski *et al.,* 2006); see Figure 6. Across the United States-Mexico border, in southwestern Arizona fast polarization directions are also oriented ENE-WSW but these gradually rotate to NE-SW as one moves towards central, northern, and eastern Arizona (Ruppert, 1992; G. Zandt, COARSE deployment, University of Arizona, unpublished data, 2004; Fouch and Gilbert, 2007; Hongsresawat *et al.,* 2015). Broadly speaking, the ENE-WSW fast axes observed in the WMBR are aligned in the same direction as the APM of North America, which is oriented ~N254°E (Gripp and Gordon, 2002); Figure 6. Additionally, the ENE-WSW fast polarization directions are also oriented with the regional extension direction during the Miocene (Sedlock *et al.,* 1993 and references therein). In the latest Miocene, as rifting started along the axis of the modern Gulf of California, the extension direction changed to its current configuration which is roughly NW-SE (Sedlock *et al.,* 1993 and references therein). Based on the previous arguments, Obrebski *et al.* (2006) and van Benthem *et al.* (2008), proposed that both mechanisms are responsible for the observed anisotropy. The APM mechanism implies that the rigid lithosphere drags the asthenosphere beneath and aligns the olivine crystals in the upper mantle (Silver, 1996). On the other hand, fossil anisotropy would have been preserved since the Miocene in the lithosphere. Fossil anisotropy has also been proposed in the Northern Basin and Range (Great Basin of Nevada) as a consequence of extension, even as present-day extension is occurring in a different direction (Savage *et al.,* 1990). These two explanations for the observed anisotropy are not mutually exclusive, and in fact suggest that anisotropy is coherent in the lithosphere and the asthenosphere. Long (2010) also studied anisotropy in the WMBR. She proposed that anisotropy in two of her NARS-Baja California stations is controlled by the APM of North America, which is consistent with O06 and B08. In their work, however, O06 and B08 had access to permanent stations which were not available to Long (2010). Therefore O06 and B08 proposed that the APM mechanism acts over a larger area. In the paper by Long (2010), null measurements in the northernmost NARS WMBR station is explained as a local effect which is dominant over the APM. Long (2010) suggested that under this station mantle flow is vertical as a consequence of an upwelling center in the Delfín Basin as documented by Wang *et al.* (2009).

Northern and Northeastern Mexico

Seismic stations in northern Mexico are sparse. Figure 5a shows the available **KS* measurements. CGIG is the northernmost station within this region. Its fast polarization direction runs NE-SW (Ponce-Cortés, 2012). This direction stands in contrast with the ENE-WSW fast axes of stations in the WMBR located to the south and southwest (Figure 5a). It is also different from the roughly NW-SE fast axes of stations HPIG and ZAIG located to the south-southeast (Figure 5a). Station CGIG is located south of New Mexico state across the Mexican border with the United States. Shear wave splitting measurements using data from the USArray Transportable Array (TA) in southwestern New Mexico show fast polarization directions oriented NE-SW to NNE-SSW (Refayee *et al.,* 2014; Hongsresawat *et al.,* 2015) and seem to be broadly consistent with the fast axis at CGIG. Refayee *et al.* (2014) proposed that anisotropy in western New Mexico and southern and eastern Texas is controlled by the edge of the North American craton. As the lithospheric continental root moves southwest, it drives asthenospheric flow around the western edge of the craton, then around the southern edge, and finally around the southeastern edge (Figure 9 in Refayee *et al.,* 2014). The southernmost edge of the North American craton is not well defined seismically due to a lack of data in Mexico, but it seems to extend under northeastern Chihuahua and northern Coahuila (Burdick *et al.,* 2012; Refayee *et al.,* 2014). Geologic and seismic evidence for the location of the southeastern edge of the craton seem to agree. The seismically defined edge of the craton (Refayee *et al.,* 2014) is consistent with the location of the Ouachita-Marathon orogenic belt in Arkansas and eastern and south-central Texas (Sedlock *et al.,* 1993 and references therein). The continuation of the Ouachita-Marathon system in Mexico is not clear, but it is agreed that, within the limitations of the data, it should be in northern Chihuahua and Coahuila (Sedlock *et al.,* 1993 and references therein). Given the similarities between the fast axis at CGIG and the fast axes in southwestern New Mexico, and the plausible location of the southernmost edge of the North American craton in northern Mexico, it is proposed in the present study that the orientation of the fast axis at CGIG is controlled by asthenospheric mantle flow around the edge of the craton. It is hoped that the availability of new data in the future will provide a sharper image of anisotropy in this region.

The fast polarization directions at stations HPIG, ZAIG, and LNIG in northern and northeastern Mexico are aligned WNW-ESE to NW-SE (van Benthem, 2005; Ponce-Cortés, 2012; van Benthem *et al.,* 2013) and are different from the orientation of the fast axes at all other stations in Mexico (Figure 5a). Stations HPIG and ZAIG are roughly located at the intersection of the Sierra Madre Occidental and the Eastern Mexican Basin and Range, or EMBR (Ortega-Gutiérrez *et al.,* 1992). The seismic fast axes at these two stations are oriented with the trend of the SMOc. The SMOc represents a coherent block which has not undergone significant extension and deformation, flanked to the west by the WMBR, and to the east by the EMBR. Both the western and eastern Mexican Basin and Range are extensional domains and are the southern continuation of the Basin and Range (BR) province of the southwestern United States (Henry and Aranda-Gomez, 1992; Sedlock *et al.,* 1993). The WMBR and the EMBR are characterized by north-northwest-elongate basins and ranges, similar to the province in the United States (Henry and Aranda-Gomez, 1992). ENE-WSW extension started as early as 30 Ma and continues to the present (Henry and Aranda-Gomez, 1992). At this point a comparison will be made with the Colorado Plateau (CP) and the Basin and Range of the United States. Like the SMOc in Mexico, the CP is a region that has not been subjected to extension and deformation (Savage and Silver, 1993; Levander *et al.,* 2011) but it is surrounded by a Cenozoic extensional regime to the west and south in the BR, and to the east in the Rio Grande Rift (Savage and Sheehan, 2000 and references therein). Shear wave splitting measurements have found seismic fast axes parallel to the western and northern boundaries of the CP (Savage and Silver, 1993; Sheehan *et al.,* 1997). Savage and Silver (1993) proposed that the contrast in physical properties such as heat flow anomalies, gravity and magnetic anomalies, and crustal thickness between the plateau and the surrounding extensional regions tends to align the seismic fast axes parallel to the plateau boundary. In the present study it is suggested that the situation between the CP and adjacent BR is similar to the one observed between the SMOc and the EMBR, thus providing the same mechanism to explain boundary-parallel fast axes in Mexico. The new SSN station PDIG is located between HPIG and ZAIG and in their same tectonic environment, so an interesting test of this hypothesis will be to determine whether the fast axes are consistently oriented at all three stations. It should also be mentioned that the fast axis at CGIG is oriented differently from the fast axes at HPIG and ZAIG (Figure 5a) even as the three stations are located in a similar tectonic environment.

The fast axis at station LNIG is oriented WNW-ESE (Ponce-Cortés, 2012); see Figure 5a. The nearest shear wave splitting measurements are found across the international border with the United States and are not consistent with the direction at LNIG. Fast polarization directions in eastern Texas, near the coast of the Gulf of Mexico, are oriented roughly NE-SW to ENE-WSW (Gao *et al.,* 2008; Satsukawa *et al.,* 2010; Refayee *et al.,* 2014; Hongsresawat *et al.,* 2015) and with the APM of North America. Station LNIG is located ~40 km east of the Sierra Madre Oriental (SMOr) in a wide transition zone between the SMOr and the Gulf of Mexico Coastal Plain (Ramos-Zuñiga *et al.,* 2012). The SMOr is made up of a sequence of carbonate and clastic marine sedimentary rocks of Late Jurassic and Cretaceous ages which were complexly folded and overthrusted during the Laramide orogeny (Ramos-Zuñiga *et al.,* 2012 and references therein). In the region between Monterrey and Veracruz, Laramide shortening occurred in the Late Paleocene to Middle Eocene, i. e. from about 57 to 46 Ma (Sedlock *et al.,* 1993 and references therein). Shortening was oriented ENE-WSW to NE-SW and produced a foreland fold and thrust belt trending roughly NNW-SSE (Sedlock *et al.,* 1993 and references therein). The Gulf Coastal Plain is a thick sequence of clastic sediments of Tertiary age characterized by extensional deformation (Ramos-Zuñiga *et al.,* 2012 and references therein). The most obvious structural feature near LNIG is theSMOr. Based on the VCD model (Silver, 1996) of lithospheric deformation during orogenies, transpressional structures are expected to produce strike-parallel fast axes. Yet, the WNW-ESE fast axis at LNIG is oriented oblique (~45°) to the NNW-SSE trend of the SMOr. So, the available evidence does not suggest that the compression which created the SMOr is responsible for the fast polarization direction measured at LNIG. Maybe station LNIG is far enough away from the SMOr that other, unknown factors control its anisotropy. Hopefully, future shear wave splitting measurements at the new SSN stations MNIG and GTIG, north-northwest and south-southeast of LNIG, respectively, will shed light on this issue. These stations are also located near the SMOr.

The Mexican Middle America Trench

In the Mexican segment of the Middle America Trench, the oceanic Rivera and Cocos plates subduct under the continental North American plate (Figure 7a). The Rivera plate is located at the western end of the trench and moves at a relative velocity which increases from 1.7 cm/yr in the northwest to 2.9 cm/yr in the southeast according to model PVEL (DeMets *et al.,* 2010); see Figure 7a. It moves in the direction ~N35°E. The larger Cocos plate is located southeast of the Rivera plate and moves at a faster relative velocity. Its velocity increases from 5.1 cm/yr in the northwest to 7.3 cm/yr in the southeast in the direction ~N31°E. The Rivera slab subducts at an angle between ~50° (Pardo and Suárez, 1993, 1995) and 60-65° (Yang *et al.,* 2009) which is actually steeper than the adjacent Cocos slab. This segment of the Cocos slab dips at ~30° (Pardo and Suárez, 1995) to ~40° (Dougherty *et al.,* 2012). Between the MAT and the coastline, the boundary between the Cocos and Rivera plates is continued by the bathymetric feature known as El Gordo Graben, which further extends on land as the N-S trending Colima rift. A gap between the Rivera and Cocos slabs was imaged tomographically at depths greater than 150 km (Yang *et al.,* 2009). Towards the east, it has been proposed (Bandy, 1992; Bandy *et al*., 2000; Dougherty *et al*., 2012) that the Cocos slab is fragmenting into a North Cocos plate and a South Cocos plate along the projection of the Orozco Fracture Zone (OFZ). The slab dip angle changes abruptly across this tear in the Cocos slab from ~40° in the west side to ~25° in the east (Dougherty *et al.,* 2012). Based on fundamental mode Rayleigh wave phase velocity dispersion measurements, Stubailo *et al.* (2012) also argue for the existence of a tear in the Cocos slab underneath the projection of the OFZ. Farther east still, a region of flat slab subduction is encountered (Pardo and Suárez, 1995; Pérez-Campos *et al.,* 2008; Husker and Davis, 2009). Dougherty and Clayton (2014) presented evidence for a possible slab tear within the subducted South Cocos plate near the abrupt eastern termination of the Trans-Mexican Volcanic Belt (TMVB). They observed an abrupt dip change from ~10° in the west side to ~25° in the east across this proposed tear in the slab. Other researchers established earlier that the slab dips at ~25° on the eastern side (Pardo and Suárez, 1995; Rodríguez-Pérez, 2007; Melgar and Pérez-Campos, 2011; Kim *et al.,* 2011). Based on a receiver function study and on isodepth seismicity patterns, Rodríguez-Domínguez (2016) proposed that the rupture may possibly be at an early stage of development. Fasola *et al.* (2016) argue that the slab is not torn in the updip region. They propose instead that the transition from flat to steeper subduction occurs rapidly via a sharp flexure. Going farther east still, the Tehuantepec Ridge (TR) intersects the MAT. The TR has long been recognized as a sharp contrast in the properties of the Cocos plate. The oceanic crust of the Guatemala Basin in the southeast is older and deeper than the region northwest of the TR; see Manea *et al.* (2005) for a review. The Tehuantepec Ridge is extended onshore under the North American plate (Manea and Manea, 2008). By the time the Cocos slab reaches the Mexico-Guatemala border it subducts even more steeply at 45° (Rodríguez-Pérez, 2007).

Most studies of upper mantle anisotropy in the MAT have involved teleseismic, core-transmitted **KS* phases recorded by stations in Mexico as reviewed below. These have shown predominantly trench-perpendicular fast polarization directions, which are often interpreted as the result of subslab entrained flow. The source-side splitting study by Lynner and Long (2014a) stands out because they used teleseismically recorded *S* waves from intraslab earthquakes in Mexico in order to sample subslab anisotropy in Mexico. One advantage of the method is the use of events at epicentral distances between 40 and 80°, thus increasing the number of events that can be used for shear wave splitting measurements (relative to studies limited to the use of core-transmitted **KS* phases at distances greater than 85°). It is necessary to account for anisotropy beneath the station. Corrections are obtained from previous **KS* measurements at the stations. It is best to use stations where no anisotropy has been detected, or else stations that show a simple pattern that can be characterized by a single anisotropic layer (Lynner and Long, 2014a). Another advantage of the method, compared to **KS* studies, is that subslab anisotropy can be quantified without the need to account for anisotropy in the mantle wedge and the overriding plate (Lynner and Long, 2014a). Lynner and Long (2014a) applied the source-side splitting technique to subduction in Central America, including Mexico. They obtained plate motion-parallel (i. e. approximately trench-perpendicular) fast polarization directions along the entire length of the MAT. For the specific case of Mexico, their results of subslab anisotropy are consistent with the **KS* studies to be reviewed in here.

Teleseismic shear wave splitting measurements in the Rivera segment of the MAT are shown in Figures 7b and 8. Under the Rivera slab (area between the western and central polygons in Figure 8), the fast axes are oriented in the direction of relative plate motion between the Rivera and North American plates (i. e., trench-perpendicular) and are thus interpreted to result from both subslab entrained flow and from corner flow in the mantle wedge (León Soto *et al.,* 2009). The fast axes of the three stations in the western polygon (Figure 8) are oriented in a semi-circular pattern around the western edge of the Rivera slab. These orientations are clearly different from those in the adjacent stations to the east. León Soto *et al.* (2009) proposed that this pattern shows slab rollback driving mantle flow around the slab edge from beneath the slab into the mantle wedge. The central polygon (Figure 8) shows yet a different pattern of fast polarization directions for stations within the Colima rift. León-Soto *et al.* (2009) pointed out that the pattern is

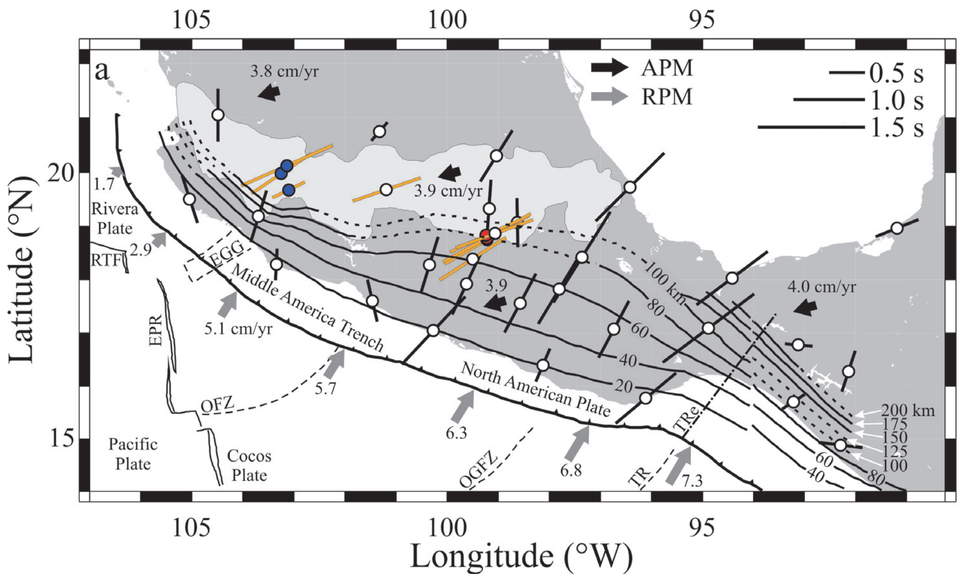

Figure 7a. Station-averaged splitting parameters in southern Mexico. The length of the bars is proportional to δt, as indicated in the legend. White dots represent SSN permanent stations (van Benthem, 2005; Ponce-Cortés, 2012; van Benthem *et al.,* 2013). (a) Blue dots are for MARS stations (León Soto *et al.,* 2009) and red dots stand for the MASE array (Rojo-Garibaldi, 2011; Bernal-López, 2015; Bernal-López *et al.,* 2016). Orange bars indicate stations where the fast polarization direction is oriented with the APM of North America. Black arrows indicate the direction of absolute plate motion (APM) for North America (Gripp and Gordon, 2002). Gray arrows show the direction of the relative plate motion (RPM) of both the Rivera and Cocos plates with respect to North America (DeMets *et al.,* 2010). RPM velocities are given in cm/yr. The Middle America Trench is represented by the line with small triangles. The Trans-Mexican Volcanic Belt (TMVB) is indicated by the light shading. Solid lines represent the isodepth contours of hypocenters within the subducting Rivera and Cocos plates. Lines are dashed where no hypocenters were available. Contours west of 94°W are from Pardo and Suárez (1995) while contours east of 94°W are from Rodríguez-Pérez (2007). In all cases, contours deeper than 100 km are from Rodríguez-Pérez (2007). Also shown are the Rivera Transform Fault (RTF), East Pacific Rise (EPR), El Gordo Graben (EGG), Orozco Fracture Zone (OFZ), O'Gorman Fracture Zone (OGFZ), and Tehuantepec Ridge (TR). TRe represents the extension of the Tehuantepec Ridge as subducted under the North American plate, from Manea and Manea (2008).

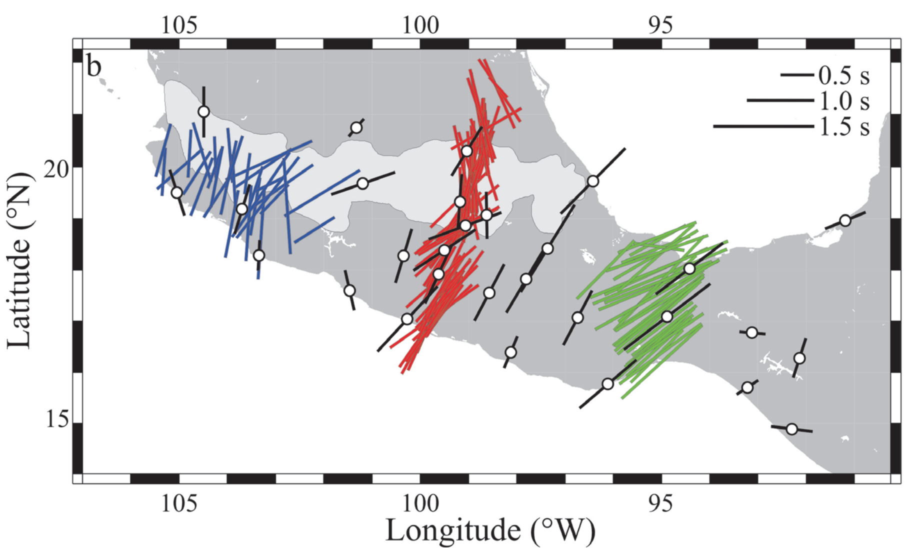

Figure 7b. (b) Same data as Figure 7a, but data from the following temporary arrays were added: blue bars represent MARS stations (León Soto *et al.,* 2009), red bars are for MASE stations (Rojo-Garibaldi, 2011; Bernal-López, 2015; Bernal-López *et al.,* 2016), and green bars stand for the VEOX deployment (Bernal-Díaz *et al.,* 2008; G. León Soto and R. W. Valenzuela, manuscript in preparation, 2017). No dots were plotted to avoid crowding the figure.

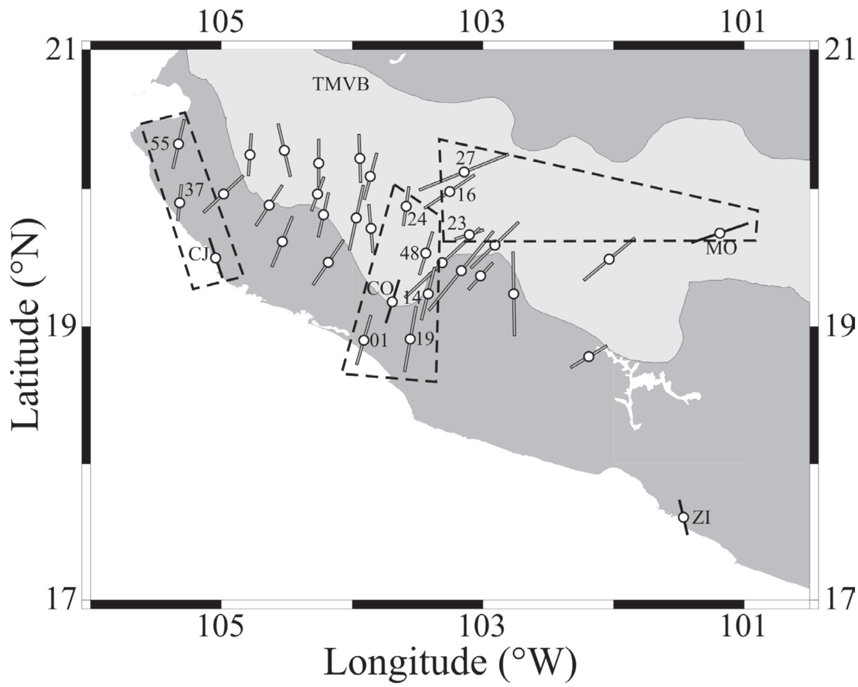

Figure 8. Station-averaged splitting parameters in the Rivera segment of the MAT. Filled bars represent SSN stations (van Benthem, 2005; León Soto *et al.,* 2009; van Benthem *et al.,* 2013) and empty bars stand for MARS stations (León Soto *et al.,* 2009). The stations enclosed by dashed-line polygons are discussed in the main text. MARS station codes were shortened by dropping the MA- prefix. The -IG suffix was dropped from SSN stations. Figure from van Benthem *et al.* (2013).

consistent with mantle flow through the slab gap between the Rivera and Cocos plates, and perhaps controls the location of Colima volcano within the rift (Yang *et al.,* 2009). Ferrari *et al.* (2001) documented rollback of the Rivera plate based on the trenchward migration of the volcanic front and further proposed asthenospheric infiltration into the mantle wedge from both the western and eastern edges of the subducted Rivera slab. Recent results of laboratory, analog models reveal complex patterns of toroidal flow between the Rivera and Cocos slabs (Neumann *et al.,* 2016) which agree with the anisotropy observations of León-Soto *et al.* (2009). In addition to using teleseismic data, León-Soto *et al.* (2009) also made shear wave splitting measurements with the MARS dataset using local, intraslab earthquakes in the depth range between 60 and 105 km as their sources. The paths from these hypocenters only sample the slab itself, the mantle wedge, and the continental crust, thus avoiding the subslab mantle altogether. They concluded that their results likely reflected anisotropy in the continental crust, with little contribution from the mantle wedge.

One single station is located where the subducted Orozco Fracture Zone meets the continent and where the tear between the North and South Cocos slabs has been proposed (station at the coastline at 101.5°W longitude in Figure 7a). The fast polarization direction at this station is clearly different from the fast axes to the east where the Cocos slab subducts subhorizontally (van Benthem, 2005; van Benthem *et al.,* 2013). Stubailo *et al.* (2012) interpreted the anisotropy patterns in their Rayleigh wave data in terms of toroidal mantle flow around the slab edges driven by slab rollback (Ferrari, 2004). The **KS* orientation of the fast axis at this single station shows that the direction of mantle flow is different from that at stations farther east and may be compatible with flow through the North Cocos-South Cocos slab gap. However, measurements from new, additional stations in this region are required in order to confirm this observation.

In the segment of the MAT between 96 and 101°W longitude the Cocos slab subducts subhorizontally (Pardo and Suárez, 1995;

Pérez-Campos *et al.,* 2008; Husker and Davis, 2009). In the fore-arc (i. e., the region between the shoreline and the TMVB) the fast polarization directions are oriented NE-SW, which is convergence-parallel, or trench-perpendicular. SSN stations afford good coverage of the area (van Benthem, 2005; Ponce-Cortés, 2012; van Benthem *et al.,* 2013); see Figure 7a. Additionally, this was the site of the dense MASE profile which ran north from Acapulco, through the TMVB, and farther north nearing the Gulf of Mexico (Stubailo and Davis, 2007, 2012a, 2012b, 2015; Rojo-Garibaldi, 2011; Bernal-López, 2015; Stubailo, 2015; Bernal-López *et al.,* 2016); see Figure 7b. Given the flat geometry of the slab, splitting measurements sample the subslab mantle flow. Physical conditions beneath the slab are expected to be low stress, low water content, and relatively high temperature, and so A-type olivine is predicted (Jung *et al.,* 2006; Long and Silver, 2008). Therefore, entrained subslab mantle flow and strong coupling between the slab and the subslab mantle are inferred (van Benthem *et al.,* 2013; Bernal-López *et al.,* 2016). The modern, active volcanic arc is located at the southern end of the TMVB (Macías, 2005). Under the TMVB the Cocos slab steepens abruptly and dips at ~75°, reaching a maximum depth of ~500 km (Pérez-Campos *et al.,* 2008; Husker and Davis, 2009; Kim *et al.,* 2010). Additionally, the TMVB is not subparallel to the offshore trench (Gill, 1981; Suarez and Singh, 1986; Ferrari *et al.*, 2012). In the back-arc (i. e., the region north of the TMVB and the northern TMVB) the seismic fast axes change orientation and align N-S, which is perpendicular to the strike of the steeply dipping slab (Rojo-Garibaldi, 2011; Ponce-Cortés, 2012; Bernal-López, 2015; Bernal-López *et al.,* 2016); see Figure 7b. This is true for the northern half of the MASE array and two nearby SSN stations. B-type olivine is frequently observed in the mantle wedge tip worldwide (Kneller *et al.,* 2005; Jung *et al.,* 2006; Long, 2013). In this particular segment of the Mexican subduction zone, however, high temperatures, in excess of 900°C, exist throughout the mantle wedge and dehydration of the slab occurs down to depths of 150 km (Manea and Manea, 2011). Therefore, Bernal-López *et al.* (2016) inferred that C-type olivine is present in the wedge tip. Physical conditions in the mantle wedge core usually are low stress, low water content, and relatively high temperature and so the existence of A-type olivine is expected (Kneller *et al.,* 2005; Jung *et al.,* 2006; Long and Silver, 2008). For both A- and C-type olivine, the fast axes align in the direction of mantle flow. Bernal-López *et al.* (2016) concluded that the N-S axes result from slab strike-perpendicular, 2-D corner flow in the mantle wedge, and also that the downgoing slab and the mantle around it are strongly coupled.

Stubailo (2015) also made shear wave splitting measurements using *SKS* and *SKKS* phases recorded by the MASE array. His results will be discussed here. For this purpose, it should be mentioned that the MASE splitting results in Figure 7b showing NE-SW fast axes in the fore-arc, and N-S axes in the back-arc were made from *SKS* phases only (Figure 5a in Bernal-López *et al.,* 2016). Measurements that only use *SKKS* phases do not show the N-S fast axes in the back-arc (Figure 5b in Bernal-López *et al.,* 2016). Instead, their *SKKS*-only measurements are consistently oriented NE-SW all along the array. The reasons for this discrepancy are discussed at length by Bernal-López *et al.* (2016). The possible causes are (1) back azimuthal dependence, perhaps an indication that two or more anisotropic layers are present under the station. (2) Differing paths to stations located at the southern and northern ends of the array, such that some rays could go through the steeply dipping slab, while others could avoid it altogether. (3) Anisotropy in the lowermost mantle as described by Long (2009a) from *SKKS* measurements at back azimuths roughly coincident with the *SKKS* observations of Bernal-López *et al.* (2016). In any case, measurements by Stubailo (2015) using both *SKS* and *SKKS* phases show fast axes mostly oriented NE-SW, in the range between N30°E and N60°E, for the entire length of the MASE array. In this regard, his results are more consistent with the *SKKS*-only measurements of Bernal-López *et al.* (2016). Stubailo (2015) stated that the NE-SW fast axes observed at the MASE array, and also at SSN stations east of MASE, are oriented in the APM direction for North America. Additionally, Stubailo *et al.* (2012), and also Stubailo (2015), made fundamental mode Rayleigh wave phase velocity dispersion measurements including anisotropy. They created a 3-D model extending down to 200 km depth. The model is made up of three layers: the continental crust, a mantle lithosphere about 50 to 60 km thick, and an asthenosphere 100 km thick. The surface wave seismic fast axes within the mantle lithosphere and the asthenosphere in the fore-arc, near the MASE stations, are oriented trench-parallel, which is inconsistent with the splitting directions. Taking into account the surface wave anisotropy pattern in the top 200 km of the Earth and the poor depth resolution afforded by shear wave splitting measurements, Stubailo (2015) proposed that the **KS* anisotropy was located deeper than

200 km. In a further step, Stubailo (2015) determined phase velocities of higher mode Rayleigh waves because overtones sample the deep structure that is poorly sampled by the fundamental mode. The higher mode phase velocity patterns, together with the sensitivity kernels, tentatively suggested that the anisotropy determined from shear wave splitting is located at depths of 200 to 400 km. The 200-400 km depth likely corresponds to the bottom of the asthenosphere, and it may be affected by the plate motion, explaining why the fast shear wave splitting direction is aligned with the plate motion of North America (Stubailo, 2015).

Between 94 and 96°W longitude, the teleseismic fast polarization directions show a slight clockwise rotation of ~25° relative to stations located over the subhorizontal slab to the west. Figure 7a shows measurements at three SSN stations (van Benthem, 2005; Ponce-Cortés, 2012; van Benthem *et al.,* 2013). Additional **KS* measurements from the VEOX array confirm the orientation of the fast axes (Bernal-Díaz *et al.,* 2008; Valenzuela-Wong *et al.,* 2015; G. León Soto and R. W. Valenzuela, manuscript in preparation, 2017); see Figure 7b. In addition to the possible tear in the slab and the change from flat to steeper subduction (Dougherty and Clayton, 2014) which were discussed above, other changes in subduction zone morphology take place here. (1) The MAT makes a bend around 96°W longitude and becomes oriented NW-SE. (2) The Tehuantepec Ridge intersects the MAT (Manea *et al.,* 2005) as previously discussed. (3) The coastline is farther away from the MAT than in the area located to the west, which implies the existence of a broad continental shelf. This is also the site where the enigmatic Yucatán slab was imaged in VEOX receiver functions (Kim *et al.,* 2011, 2014). It has been suggested that the Yucatán slab is a southwest-dipping structure opposing, and in fact cutting through, the long-recognized northeast-dipping Cocos slab (Kim *et al.,* 2011). In spite of the change in the **KS* fast polarization directions, these are still reasonably close to trench-perpendicular and are indicative of subslab entrained flow. The rotation of the fast polarization directions may be caused by the change in dip of the slab, the bend in the MAT, or perhaps by flow between the two edges of the (possibly) torn slab. Definitive settlement of this question may have to await for measurements from new stations in the area. It should also be noted that the orientation of the teleseismic fast axes shows a progressive clockwise rotation from the area of flat subduction to the west, to this area of steeper subduction, and finally to the Yucatán peninsula farther east (Figure 5a). The study by León Soto and Valenzuela (2013) also relied on VEOX data in the Isthmus of Tehuantepec. They made shear wave splitting measurements using *S* waves from deep, local intraslab earthquakes to constrain the characteristics of flow in the mantle wedge. They found that the orientations of the fast polarization directions can be divided into two regions, separated by the 100 km isodepth contour of the Cocos slab. The region southwest of the 100-km contour does not show a coherent pattern in the fast polarization directions. Given that for the shallower events the source-to-station paths through the mantle wedge are short, the anisotropy pattern may reflect a significant contribution from the overlying continental crust (León Soto and Valenzuela, 2013). To the northeast of the 100-km contour, the fast polarization directions are oriented on average N35°E and are trench-perpendicular. These measurements sample the mantle wedge core, where physical conditions are high temperature, low stress, and low water content and consequently the development of A-type olivine is expected. The observations are thus interpreted as 2-D corner flow driven by the downdip motion of the slab (León Soto and Valenzuela, 2013). Furthermore, the fast polarization directions obtained from local *S* waves are roughly consistent with the directions of the fast axes observed from **KS* phases as discussed above for this region. Taken together, the studies of van Benthem *et al.* (2013) and León Soto and Valenzuela (2013) are consistent with entrained flow under the Cocos slab.

The anisotropy pattern at the eastern end of the Mexican MAT is markedly different from that observed to the west and discussed above. These two regions are separated by the continuation of the Tehuantepec Ridge within the subducted Cocos plate. Between 92 and 94°W longitude, delay times are consistently small ($\delta t \leq 0.6$ s) and the fast axes are oriented in different directions, which is an indication of little anisotropy (Ponce-Cortés, 2012; van Benthem *et al.,* 2013); see Figure 7a. Given the nearly vertical incidence angles used for shear wave splitting measurements, these are only sensitive to the horizontal component of mantle flow. So, it is conceivably possible that mantle flow in this region is vertical, maybe within the mantle wedge, rather than beneath the slab. Since depth resolution of **KS* measurements is poor, however, it is hard to localize the depth of the observed anisotropy. Long and Silver (2008) proposed that in the mantle wedge, if neither 2-D corner flow nor 3-D flow driven by trench migration is dominant, then the competing effects of the two result in an incoherent flow regime, which may be characterized by small δt values. The Yucatán slab is also inferred to exist in this region (Kim *et al.,* 2011, 2014). Receiver function images suggest that the Yucatán slab cuts off the Cocos slab and is thus expected to hinder 2-D mantle wedge flow for both systems (Kim *et al.,* 2011). Furthermore, Kim *et al.* (2011) proposed that 3-D flow should be important. Yet another possibility is that the region of little anisotropy beneath Chiapas is transitional between the trench-perpendicular fast axes underneath Guerrero and western Oaxaca, and the region of trench-parallel axes observed farther east along the MAT under Nicaragua and Costa Rica. Abt *et al.* (2009, 2010) reported trench-parallel fast polarization directions and mantle flow in both the mantle wedge and in the subslab mantle beneath Nicaragua and Costa Rica. This view, however, is complicated by the fact that Lynner and Long (2014a), using the source-side technique, found trench-perpendicular fast axes in the subslab mantle in the same segment of the MAT. In order to explain this discrepancy, Lynner and Long (2014a) proposed that the *S* raypaths in their study and the **KS* paths in the work by Abt *et al.* (2010) sample different volumes of the subslab mantle.

Stations Consistent With the Absolute Plate Motion of North America

As previously discussed, in the model of simple asthenospheric flow, the rigid lithosphere drags the asthenosphere beneath and drives mantle flow in the same direction as APM (Silver, 1996). This mechanism has been successful at explaining fast polarization directions in tectonically stable environments of the United States (e. g. Fouch *et al.,* 2000; Refayee *et al.,* 2014; Hongsresawat *et al.,* 2015). In Mexico, the case of fast polarization directions oriented with the APM of North America in the Western Mexican Basin and Range was discussed in section 4.2. A few other examples exist in Mexico. The absolute motion of the North American plate throughout southern Mexico is about 4 cm/yr and is oriented in a direction ~N254°E according to model HS3-NUVEL1A in Gripp and Gordon (2002); see Figure 7a. In easternmost Mexico, in the Yucatán peninsula, three SSN stations show fast axes oriented ENE-WSW and are aligned in the direction of North America APM (Ponce-Cortés, 2012; van Benthem *et al.,* 2013); see Figure 5a. For these stations the APM mechanism seems rather appropriate because they are located away from any modern plate boundaries (e. g., Cocos-North America or North America-Caribbean) and the MAT, and also from ancient collision zones (vertically coherent deformation).

Starting with early studies (van Benthem, 2005; van Benthem and Valenzuela, 2007; van Benthem *et al.,* 2013), seismic fast axes oriented in the direction of North America APM were found for three SSN stations inside or just south of the TMVB (orange bars and white circles in Figure 7a). Likewise, three MARS stations within the TMVB (León Soto *et al.,* 2009; van Benthem *et al.,* 2013) have their fast axes oriented in the direction of North America APM (eastern polygon in Figure 8, and orange bars and blue circles in Figure 7a). Additionally, three MASE stations at the southern end of the TMVB (Rojo-Garibaldi, 2011; Bernal-López *et al.,* 2016) have fast axes oriented in the direction of North America APM (orange bars and red circles in Figure 7a). In spite of the wide spacing in the location of these stations (their locations range from ~99 to ~103°W longitude) they share the fact that they are located within or just south of the TMVB. They also appear to be anomalous in the orientation of their fast axes when compared with most of the other nearby stations. It may be that these stations are far enough away from the MAT that they can escape the effects of subduction zone-related mantle flow and instead respond to APM. Yet, it is intriguing that most of the adjacent stations have their fast axes orientations and mantle flow controlled by subduction processes. Furthermore, while the stations are located on the North American plate, the subducted Cocos plate is found below and should have a dominant effect on asthenospheric flow.

Lowermost Mantle Anisotropy Observed With Stations in Mexico

All through the present review, *SKS* and *SKKS* measurements in Mexico have been interpreted to result from upper mantle anisotropy. The poor depth resolution of shear wave splitting measurements, however, must not be forgotten. A look at the work by Long (2009a) is instructive because she used stations in Mexico and found an anisotropic region in the lowermost mantle. So, a word of caution is warranted in order to avoid misinterpreting lower mantle anisotropy to the upper mantle. Simultaneous measurements of *SKS* and *SKKS* shear wave splitting from the same source and station usually return the same splitting parameters (ϕ, δt) because their raypaths converge in the uppermost mantle under the station. Long (2009a) identified 15 source-to-station pairs whereby the splitting parameters determined using *SKS* waves were different from the parameters obtained from *SKKS* phases. Three stations were located in southwestern California, five belonged to the NARS-Baja California deployment in northwestern Mexico, and the last one was Geoscope station UNM (which is co-located with SSN station CUIG). The anomalous measurements were detected only for back azimuths oriented to the west and west-northwest. In most cases the *SKS* measurements returned null values, while the *SKKS* observations showed clear splitting. Given that the source-to-station paths of *SKS* and *SKKS* phases differ the most in the D" layer at the base of the mantle, Long (2009a) concluded that the anisotropy must be located there, instead of in the upper mantle. Analysis of the region sampled by the *SKKS* phases showed that anisotropy was located in a patch of D" beneath the eastern Pacific Ocean, and that it could be explained by a fragment of the Farallon slab subducted all the way down to the base of the mantle (Long, 2009a). It should also be mentioned that the anomalous *SKKS* observations are not distributed uniformly throughout the region as they are interspersed with normal *SKKS* measurements (Long, 2009a).

Conclusions

One important reason for the study of seismic anisotropy is that it provides a means to determine the direction of upper mantle flow and its relationship to tectonic processes. Mexico has a wide variety of tectonic environments. Some of them are currently active whereas others were active in the past. In either case, tectonic processes often leave a signature in the upper mantle in the form of seismic anisotropy. It is the purpose of this paper to present a review and summary of the different studies of upper mantle shear wave splitting conducted in Mexico during the last decade. Fast polarization directions in the northern half of the Baja California peninsula are oriented E-W and result from subduction of the former Farallon plate. In the southern half of the peninsula anisotropy is weak. Given that the shear wave splitting technique is only sensitive to the horizontal component of mantle flow, the observed anisotropy pattern may be consistent with vertical upwelling produced by the former Magdalena ridge. Measurements from one single station at the southernmost tip of Baja California are more consistent with anisotropy in the northern half of the peninsula and may be related to the angle of subduction of the former Farallon plate. In the Western Mexican Basin and Range the fast polarization directions are oriented ENE-WSW and are aligned with the APM of North America and also with the direction of extension during the Miocene. The origin of anisotropy may be both, current in the asthenosphere, and fossil in the lithosphere. Stations in northern Mexico are few and far between. One station in northern Chihuahua state has the fast axis oriented NE-SW and is consistent with observations across the United States border. Its anisotropy pattern seems to be controlled by asthenospheric mantle flow around the southern edge of the North American craton. A couple of stations are roughly located at the intersection of the Sierra Madre Occidental with the Eastern Mexican Basin and Range. Their fast axes are oriented NW-SE to WNW-ESE and are aligned with the trend of the SMOc. Thus, the contrast in physical properties between the underformed SMOc and the extended EMBR may orient the fast axes in the direction of the boundary between the two different tectonic provinces. The seismic fast axes for stations affected by subduction of the Rivera and Cocos plates under North America are predominantly oriented in the direction of relative plate convergence and are approximately trench-perpendicular. These are interpreted as subslab entrained flow. Also, trench-perpendicular corner flow is inferred in the mantle wedge above the Rivera plate and above the Cocos plate in eastern Oaxaca state. Flow is also interpreted to occur around the western edge of the Rivera slab and through the tear between the Rivera and Cocos slabs, consistent with the ongoing process of slab rollback. Under the fore-arc of the subhorizontal slab in Guerrero state, the NE-SW oriented fast axes are consistent with entrained subslab mantle flow. In the back-arc, north of the TMVB, the slab dips steeply and N-S fast polarization directions are consistent with slab strike-perpendicular corner flow in the mantle wedge. The fast axes of stations in the Isthmus of Tehuantepec are rotated ~25° clockwise relative to the fast axes of stations over the flat slab. Farther east, in Chiapas, the splitting parameters are indicative of weak anisotropy and may be related to disturbances in mantle flow caused by the proposed Yucatán slab. Alternatively, the fast axes there may be transitional between the trench-perpendicular fast axes beneath Guerrero and western Oaxaca, and the trench-parallel fast axes observed farther east along the MAT under Nicaragua and Costa Rica. The fast axes in the Yucatán peninsula are oriented ENE-WSW and are aligned with the APM of North America. The APM mechanism for these stations is consistent with their locations away from current plate boundaries and from former collision zones. Finally, observations in some NARS-Baja California stations and at Geoscope station UNM have been interpreted as anisotropy in the lowermost mantle in a region beneath the eastern Pacific roughly parallel to the west coast of North America. It has been suggested that these observations can be explained by the subducted Farallon slab at that depth.

Acknowledgments

We are thankful to Karen Fischer for providing the computer code to measure the splitting parameters, and for giving a seminar that sent one of us (R. W. V.) down the long "anisotropy road"; Fernando Terán for the computer code to check the measurements; Manuel Velásquez for computer support; and Vlad Manea, Marina Manea, and Rob Clayton for discussions and suggestions. The suggestions made by Raúl Castro and Takeshi Mikumo greatly enriched the manuscript. We are grateful to the following colleagues who have collaborated with us in the anisotropy studies. They are, in rough chronological order, Jeremías Basurto, Antonio Lozada, Steven van Benthem, Raúl Castro, Mathias Obrebski, Alberto Bernal, Adriana González, Berenice R. Garibaldi, Gustavo Ponce, Iliana Olarte, and Leslie Alejandra Bernal. Mexico's Servicio Sismológico Nacional (SSN) data are available through the work of its staff, which involves station maintenance, data acquisition and distribution. We also wish to thank Centro de Investigación Científica y de Educación Superior de Ensenada for access to data from their network. We are also grateful to the many people whose foresight and hard work made the NARS-Baja California, MARS, MASE, and VEOX deployments a reality. This work was partly funded by Universidad Nacional Autónoma de México through Programa de Apoyo a Proyectos de Investigación e Innovación Tecnológica, PAPIIT grant IN112814. The contour plots and maps in this study were made using the Generic Mapping Tools (GMT) package (Wessel and Smith, 1998).

References

Abt D. L., Fischer K.M., Abers G.A., Strauch W., Protti J.M., González V., 2009, Shear wave anisotropy beneath Nicaragua and Costa Rica: Implications for flow in the mantle wedge, *Geochem. Geophys. Geosyst.,* 10, Q05S15, doi:10.1029/2009GC002375.

Abt D.L., Fischer K.M., Abers G.A., Protti M., González V., Strauch W., 2010, Constraints on upper mantle anisotropy surrounding the Cocos slab from *SK*(*K*)*S* splitting, *J. Geophys. Res.,* 115, B06316, doi:10.1029/2009JB006710.

Alsina D., Snieder R., 1995, Small-scale sublithospheric continental mantle deformation: Constraints from *SKS* splitting observations, *Geophys. J. Int.,* 123, 431-448.

Ando M., 1984, *ScS* polarization anisotropy around the Pacific Ocean, *J. Phys. Earth,* 32, 179-196.

Ando M., Ishikawa Y., 1982, Observations of shear-wave velocity polarization anisotropy beneath Honshu, Japan: Two masses with different polarizations in the upper mantle, *J. Phys. Earth,* 30, 191-199.

Ando M., Ishikawa Y., Yamazaki F., 1983, Shear wave polarization anisotropy in the upper mantle beneath Honshu, Japan, *J. Geophys. Res.,* 88, 5850-5864.

Babuska V., Cara M., 1991, *Seismic anisotropy in the Earth, Modern Approaches in Geophysics,* vol. 10. Kluwer Academic Publishers, Dordrecht, The Netherlands, 217 pp.

Balfour N.J, Savage M.K., Townend J., 2005, Stress and crustal anisotropy in Marlborough, New Zealand: Evidence for low fault strength and structure-controlled anisotropy, *Geophys. J. Int.,* 163, 1073-1086, doi: 10.1111/j.1365-246X.2005.02783.x.

Balfour N.J, Cassidy J.F., Dosso S.E., 2012, Crustal anisotropy in the forearc of the Northern Cascadia Subduction Zone, British Columbia, *Geophys. J. Int.,* 188, 165-176, doi: 10.1111/j.1365-246X.2011.05231.x.

Bandy W.L., 1992, Geological and Geophysical investigation of the Rivera-Cocos plate boundary: Implications for plate fragmentation, Ph. D. thesis, 195 pp., Texas A & M University, College Station, TX, USA.

Bandy W.L., Hilde T.W.C., Yan C.-Y., 2000, The Rivera-Cocos plate boundary: Implications for Rivera-Cocos relative motion and plate fragmentation, in *Cenozoic tectonics and volcanism of Mexico, Geol. Soc. Am. Spec. Pap.*, 334, edited by H. Delgado-Granados, G. Aguirre-Díaz and J. M. Stock, 1-28, Geological Society of America, Boulder, CO, USA.

Barruol G., Hoffmann R., 1999, Upper mantle anisotropy beneath the Geoscope stations, *J. Geophys. Res.,* 104, 10,757-10,773.

Barruol G., Mainprice D., 1993, A quantitative evaluation of the contribution of crustal rocks to the shear wave splitting of teleseismic *SKS* measurements, *Phys. Earth Planet. Inter.,* 78, 281-300.

Bernal-Díaz A., Valenzuela-Wong R., Pérez-Campos X., Iglesias A., Clayton R.W., 2008, Anisotropía de la onda *SKS* en el manto superior debajo del arreglo VEOX, *Geos Boletín Informativo de la UGM,* 28, 2, 199-200.

Bernal-López L.A., 2015, Anisotropía sísmica y flujo del manto producidos por la placa de Cocos subducida en el sur de México, M. Sc. thesis, 65 pp., Centro de Sismología y Volcanología de Occidente, Universidad de Guadalajara, Puerto Vallarta, Jal., Mexico.

Bernal-López L.A., Garibaldi B.R., León Soto G., Valenzuela R.W., Escudero, C.R., 2016, Seismic anisotropy and mantle flow driven by the Cocos slab under southern Mexico, *Pure Appl. Geophys.,* 173, 3373-3393, doi:10.1007/s00024-015-1214-7.

Blackman D.K., Kendall J.M., 1997, Sensitivity of teleseismic body waves to mineral texture and melt in the mantle beneath a mid-ocean ridge, *Phil. Trans. R. Soc. Lond. A,* 355, 217-231.

Bohannon R.G., Parsons T., 1995, Tectonic implications of post-30 Ma Pacific and North American relative plate motions, *Geol. Soc. Am. Bull.,* 107, 937-959.

Boness N., Zoback M.D., 2006, Mapping stress and structurally-controlled crustal shear velocity anisotropy in California, *Geology,* 34, 825-828.

Bowman J.R., Ando M., 1987, Shear-wave splitting in the upper-mantle wedge above the Tonga subduction zone, *Geophys. J. R. Astron. Soc.,* 88, 25-41.

Burdick S., van der Hilst R.D., Vernon F.L., Martynov V., Cox T., Eakins J., Karasu G. H., Tylell J., Astiz L., Pavlis G.L., 2012, Model update March 2011: Upper mantle heterogeneity beneath North America from traveltime tomography with global and USArray Transportable Array data, *Seism. Res. Lett.,* 83, 23-28, doi:10.1785/gssrl.83.1.23.

Castro R.R., Perez-Vertti A., Mendez I., Mendoza A., Inzunza L., 2011, Location of moderate-sized earthquakes recorded by the NARS-Baja array in the Gulf of California region between 2002 and 2006, *Pure Appl. Geophys.,* 168, 1279-1292, doi:10.1007/s00024-010-0177-y.

Chen W.P., Brudzinski M.R., 2003, Seismic anisotropy in the mantle transition zone beneath Fiji-Tonga, *Geophys. Res. Lett.,* 30, 1682, doi:10.1029/2002GL016330.

Christensen N.I., 1984, The magnitude, symmetry and origin of upper mantle anisotropy based on fabric analyses of ultramafic tectonics, *Geophys. J. R. Astron. Soc.,* 76, 89-111.

Clayton R.W., Trampert J., Rebollar C., Ritsema J., Persaud P., Paulssen H., Pérez-Campos X., van Wettum A., Pérez-Vertti A., DiLuccio F., 2004, The NARS-Baja seismic array in the Gulf of California rift zone, *MARGINS Newsletter,* 13, 1-4.

Crampin S., 1994, The fracture criticality of crustal rocks, *Geophys. J. Int.,* 118, 428-438.

Crampin S., Gao, Y., 2006, A review of techniques for measuring shear-wave splitting above small earthquakes, *Phys. Earth Planet. Inter.,* 159, 1-14.

DeMets C., Gordon R.G., Argus D.F., Stein S., 1994, Effect of recent revisions to the geomagnetic reversal time scale on estimates of current plate motions, *Geophys. Res. Lett.,* 21, 2191-2194.

DeMets C., Gordon R.G., Argus D.F., 2010, Geologically current plate motions, *Geophys. J. Int.,* 181, 1-80.

Di Leo J.F., Wookey J., Hammond J.O.S., Kendall J.M., Kaneshima S., Inoue H., Yamashina T., Harjadi P., 2012, Mantle flow in regions of complex tectonics: Insights from Indonesia, *Geochem. Geophys. Geosyst.,* 13, Q12008, doi:10.1029/2012GC004417.

Dougherty S.L., Clayton R.W., 2014, Seismicity and structure in central Mexico: Evidence for a possible slab tear in the South Cocos plate, *J. Geophys. Res. Solid Earth,* 119, 3424-3447, doi:10.1002/2013JB010833.

Dougherty S.L., Clayton R.W., Helmberger D.V., 2012, Seismic structure in central Mexico: Implications for fragmentation of the subducted Cocos plate, *J. Geophys. Res.,* 117, B09316, doi:10.1029/2012JB009528.

Eakin C.M., Long M.D., Wagner L.S., Beck S.L., Tavera H., 2015, Upper mantle anisotropy beneath Peru from *SKS* splitting: Constraints on flat slab dynamics and interaction with the Nazca Ridge, *Earth Planet. Sci. Lett.,* 412, 152-162, doi:10.1016/j.epsl.2014.12.015.

Fasola S., Brudzinski M.R., Ghouse N., Solada K., Sit S., Cabral-Cano E., Arciniega-Ceballos A., Kelly N., Jensen K., 2016, New perspective on the transition from flat to steeper subduction in Oaxaca, Mexico, based on seismicity, nonvolcanic tremor, and slow slip, *J. Geophys. Res. Solid Earth,* 121, 1835-1848, doi:10.1002/2015JB012709.

Ferrari L., 2004, Slab detachment control on mafic volcanic pulse and mantle heterogeneity in central Mexico, *Geology,* 32, 77-80, doi:10.1130/G19887.1.

Ferrari L., Petrone C.M., Francalanci L., 2001, Generation of oceanic-island basalt-type volcanism in the western Trans-Mexican volcanic belt by slab rollback, asthenosphere infiltration, and variable flux melting, *Geology,* 29, 507-510.

Ferrari L., Orozco-Esquivel T., Manea V., Manea M., 2012. The dynamic history of the Trans-Mexican Volcanic Belt and the Mexico subduction zone, *Tectonophysics,* 522-523, 122-149.

Fletcher J.M., Grove M., Kimbrough D., Lovera O., Gehrels G.E., 2007, Ridge-trench interactions and the Neogene tectonic evolution of the Magdalena shelf and southern Gulf of California: Insights from detrital zircon U-Pb ages from the Magdalena fan and adjacent areas, *Geol. Soc. Am. Bull.,* 119, 1313-1336.

Foley B.J., Long M.D., 2011, Upper and mid-mantle anisotropy beneath the Tonga slab, *Geophys. Res. Lett.,* 38, L02303, doi:10.1029/2010GL046021.

Fouch M.J., Gilbert H.J., 2007, Complex upper mantle seismic structure across the southern Colorado Plateau/Basin and Range I: Results from shear wave splitting analysis, *Eos Trans. AGU,* 88, 52, Fall. Meet. Suppl., Abstract S41B-0557.

Fouch M.J., Fischer K.M., Parmentier E.M., Wysession M.E., Clarke T.J., 2000, Shear wave splitting, continental keels, and patterns of mantle flow, *J. Geophys. Res.,* 105, 6255-6275.

Gao S., Davis P.M., Liu H., Slack P.D., Zorin Y. A., 1994, Seismic anisotropy and mantle flow beneath the Baikal rift zone, *Nature,* 371, 149-151.

Gao S.S., Liu K.H., Stern R.J., Keller G.R., Hogan J.P., Pulliam J., Anthony E.Y., 2008, Characteristics of mantle fabrics beneath the south-central United States: Constraints from shear-wave splitting measurements, *Geosphere,* 4, 411-417, doi:10.1130/GES00159.1.

Gill J.B., 1981, *Orogenic andesites and plate tectonics, Minerals and rocks,* 16, Springer, Berlin, Germany.

Gripp A.E., Gordon R.G., 2002, Young tracks of hotspots and current plate velocities, *Geophys. J. Int.,* 150, 321-361.

Grupo RESNOM, 2002, Estado actual de RESNOM y sismicidad de la región noroeste de México en el periodo septiembre-diciembre de 2001 (in Spanish), *Geos Boletín Informativo de la UGM,* 22, 43-48.

Guilbert J., Poupinet G., Mei J., 1996, A study of azimuthal *P* residuals and shear-wave splitting across the Kunlun range (northern Tibetan Plateau), *Phys. Earth Planet. Inter.,* 95, 167-174.

Hecht E., 1987, *Optics, 2nd edition.* Addison-Wesley Publishing Company, Reading, MA, USA, 676 pp.

Henry C.D., Aranda-Gomez J.J., 1992, The real southern Basin and Range: Mid-to late Cenozoic extension in Mexico, *Geology,* 20, 701-704.

Hirn A., Jiang M., Sapin M., Díaz J., Nercessian A., Lu Q. T., Lepine J. C., Shi D. N., Sachpazi M., Pandy M. R., Ma K., Gallart J., 1995, Seismic anisotropy as an indicator of mantle flow beneath the Himalayas and Tibet, *Nature,* 375, 571-574.

Hongsresawat S., Panning M.P., Russo R.M., Foster D.A., Monteiller V., Chevrot S., 2015, USArray shear wave splitting shows seismic anisotropy from both lithosphere and asthenosphere, *Geology,* 43, 667-670, doi:10.1130/G36610.1.

Husker A., Davis P.M., 2009, Tomography and thermal state of the Cocos plate subduction beneath Mexico City, *J. Geophys. Res.,* 114, B04306, doi:10.1029/2008JB006039.

Jung H., Karato S.-i., 2001, Water-induced fabric transitions in olivine, *Science,* 293, 1460-1463.

Jung H., Katayama I., Jiang Z., Hiraga T., Karato S., 2006, Effect of water and stress on the lattice-preferred orientation of olivine, *Tectonophysics,* 421, 1-22.

Kaneshima S., 1990, Origin of crustal anisotropy: Shear wave splitting studies in Japan, *J. Geophys. Res.,* 95, 11,121-11,133.

Kaneshima S., 2014, Upper bounds of seismic anisotropy in the Tonga slab near deep earthquake foci and in the lower mantle, *Geophys. J. Int.,* 197, 351–368, doi:10.1093/gji/ggt494.

Kaneshima S., Ando M., Kimura S., 1988, Evidence from shear-wave splitting for the restriction of seismic anisotropy to the upper crust, *Nature,* 335, 627-629.

Karato S.-i., Jung H., Katayama I., Skemer P., 2008, Geodynamic significance of seismic anisotropy of the upper mantle: New insights from laboratory studies, *Annu. Rev. Earth Planet. Sci.,* 36, 59-95, doi:10.1146/annurev.earth.36.031207.124120.

Kim Y., Clayton R.W., Jackson J.M., 2010, Geometry and seismic properties of the subducting Cocos plate in central Mexico, *J. Geophys. Res.,* 115, B06310, doi:10.1029/2009JB006942.

Kim Y., Clayton R.W., Keppie F., 2011, Evidence of a collision between the Yucatán block and Mexico in the Miocene, *Geophys. J. Int., 187,* 989-1000, doi: 10.1111/j.1365-246X.2011.05191.x.

Kim Y., Lim H., Miller M. S., Pearce F., Clayton R. W., 2014, Evidence of an upper mantle seismic anomaly opposing the Cocos slab beneath the Isthmus of Tehuantepec, Mexico, *Geochem. Geophys. Geosyst.,* 15, 3021-3034, doi:10.1002/2014GC005320.

Kind R., Kosarev G.L., Makeyeva L.I., Vinnik L.P., 1985, Observations of laterally inhomogeneous anisotropy in the continental lithosphere, *Nature,* 318, 358-361.

Kneller E.A, van Keken P.E., Karato S.-i., Park J., 2005, B-type olivine fabric in the mantle wedge: Insights from high-resolution non-Newtonian subduction zone models, *Earth Planet. Sci. Lett.,* 237, 781-797, doi:10.1016/j.epsl.2005.06.049.

León Soto G., Valenzuela R.W., 2013, Corner flow in the Isthmus of Tehuantepec, Mexico inferred from anisotropy measurements using local intraslab earthquakes, *Geophys. J. Int.,* 195, 1230-1238, doi:10.1093/gji/ggt291.

León Soto G., Ni J.F., Grand S.P., Sandvol E., Valenzuela R.W., Guzmán Speziale M., Gómez González J. M., Domínguez Reyes T., 2009, Mantle flow in the Rivera-Cocos subduction zone, *Geophys. J. Int.,* 179, 1004-1012, doi: 10.1111/j.1365-246X.2009.04352.x.

Levander A., Schmandt B., Miller M.S., Liu K., Karlstrom K.E., Crow R.S., Lee C.-T. A., Humphreys E.D., 2011, Continuing Colorado plateau uplift by delamination-style convective lithospheric downwelling, *Nature,* 472, 461–465, doi:10.1038/nature10001.

Levin H.L., 1986, *Contemporary physical geology, 2nd edition.* Saunders College Publishing, Philadelphia, PA, USA, 558 pp.

Liu K.H., 2009, NA-SWS-1.1: A uniform database of teleseismic shear wave splitting measurements for North America, *Geochem. Geophys. Geosyst.,* 10, Q05011, doi:10.1029/2009GC002440.

Long M.D., 2009a, Complex anisotropy in D” beneath the eastern Pacific from *SKS-SKKS* splitting discrepancies, *Earth Planet. Sci. Lett.,* 283, 181-189.

Long M.D., 2009b, Going with the mantle flow, *Nat. Geosci.,* 2, 10-11.

Long M.D., 2010, Frequency-dependent shear wave splitting and heterogeneous anisotropic structure beneath the Gulf of California region, *Phys. Earth Planet. Inter.,* 182, 59-72, doi:10.1016/j.pepi.2010.06.005.

Long M.D., 2013, Constraints on subduction geodynamics from seismic anisotropy, *Rev. Geophys.,* 51, 76-112, doi:10.1002/rog.20008.

Long M.D., Becker T.W., 2010, Mantle dynamics and seismic anisotropy, *Earth Planet. Sci. Lett.,* 297, 341-354, doi:10.1016/j.epsl.2010.06.036.

Long M.D., Silver P.G., 2008, The subduction zone flow field from seismic anisotropy: A global view, *Science,* 319, 315-318, doi:10.1126/science.1150809.

Long M.D., Silver P.G., 2009a, Shear wave splitting and mantle anisotropy: Measurements, interpretations, and new directions, *Surv. Geophys.,* 30, 407-461, doi:10.1007/s10712-009-9075-1.

Long M.D., Silver P.G., 2009b, Mantle flow in subduction systems: The subslab flow field and implications for mantle dynamics, *J. Geophys. Res.,* 114, B10312, doi:10.1029/2008JB006200.

Long M.D., Wirth E.A., 2013, Mantle flow in subduction systems: The mantle wedge flow field and implications for wedge processes, *J. Geophys. Res. Solid Earth,* 118, 583-606, doi:10.1002/jgrb.50063.

Lynner C., Long M.D., 2013,Sub-slab seismic anisotropy and mantle flow beneath the Caribbean and Scotia subduction zones: Effects of slab morphology and kinematics, *Earth Planet. Sci. Lett.* 361, 367-378, doi:10.1016/j.epsl.2012.11.007.

Lynner C., Long M.D., 2014a, Sub-slab anisotropy beneath the Sumatra and circum-Pacific subduction zones from source-side shear wave splitting observations, *Geochem. Geophys. Geosyst.,* 15, 2262–2281, doi:10.1002/2014GC005239.

Lynner C., Long M.D., 2014b, Testing models of sub-slab anisotropy using a global compilation of source-side shear wave splitting data, *J. Geophys. Res. Solid Earth,* 119, 7226-7244, doi:10.1002/2014JB010983.

Macías J.L., 2005, Geología e historia eruptiva de algunos de los grandes volcanes activos de México, *Bol. Soc. Geol. Mex.,* LVII, 379-424.

Mainprice D., Silver P.G., 1993, Interpretation of *SKS*-waves using samples from the subcontinental lithosphere, *Phys. Earth Planet. Inter.,* 78, 257-280.

Manea M., Manea V.C., 2008, On the origin of El Chichón volcano and subduction of Tehuantepec Ridge: A geodynamical perspective, *J. Volcanol. Geotherm. Res.,* 175, 459-471, doi:10.1016/j.jvolgeores.2008.02.028.

Manea V.C., Manea M., 2011, Flat-slab thermal structure and evolution beneath central Mexico, *Pure Appl. Geophys.,* 168, 1475-1487, doi:10.1007/s00024-010-0207-9.

Manea M., Manea V.C., Ferrari L., Kostoglodov V., Bandy W.L., 2005, Tectonic evolution of the Tehuantepec ridge, *Earth Planet. Sci. Lett.,* 238, 64-77.

MASE, 2007, Meso America subduction experiment, Caltech, dataset, Pasadena, CA, USA, doi:10.7909/C3RN35SP.

Melgar D., Pérez-Campos X., 2011, Imaging the Moho and subducted oceanic crust at the Isthmus of Tehuantepec, Mexico, from receiver functions, *Pure Appl. Geophys.,* 168, 1449-1460, doi:10.1007/s00024-010-0199-5.

Neumann F., Vásquez-Serrano A., Tolson G., Negrete-Aranda R., Contreras J., 2016, Toroidal, counter-toroidal, and upwelling flow in the mantle wedge of the Rivera and Cocos plates: Implications for IOB geochemistry in the Trans-Mexican Volcanic Belt, *Pure Appl. Geophys.,* 173, 3395-3417, doi:10.1007/s00024-015-1218-3.

Nicolas A., 1993, Why fast polarization directions of *SKS* seismic waves are parallel to mountain belts, *Phys. Earth Planet. Inter.,* 78, 337-342.

Nicolas A., Christensen N.I., 1987, Formation of anisotropy in upper mantle peridotites: A review, in *Composition, Structure and Dynamics of the Lithosphere-Asthenosphere System, Geodyn. Ser.,* 16, edited by K. Fuchs and C. Froidevaux, pp. 111-123, AGU, Washington, D. C., USA.

Obrebski M.J., 2007, Estudio de la anisotropía sísmica y su relación con la tectónica de Baja California, Ph. D. thesis, 221 pp., Centro de Investigación Científica y de Educación Superior de Ensenada, Ensenada, B. C., Mexico.

Obrebski M., Castro R.R., 2008, Seismic anisotropy in northern and central Gulf of California region, Mexico, from teleseismic receiver functions and new evidence of possible plate capture, *J. Geophys. Res.,* 113, B03301, doi:10.1029/2007JB005156.

Obrebski M., Castro R.R., Valenzuela R.W., van Benthem S., Rebollar C.J., 2006, Shear-wave splitting observations at the regions of northern Baja California and southern Basin and Range in Mexico, *Geophys. Res. Lett.,* 33, L05302, doi:10.1029/2005GL024720.

Ortega-Gutiérrez F., Mitre-Salazar L.M., Roldán-Quintana J., Aranda-Gómez J., Morán-Zenteno D., Alaniz-Alvarez S., Nieto-Samaniego A., 1992, Carta geológica de la República Mexicana, *Fifth edition,* scale 1:2,000,000, Instituto de Geología, Universidad Nacional Autónoma de México, Mexico City, Mexico.

Özalaybey S., Savage M.K., 1994, Double-layer anisotropy resolved from *S* phases, *Geophys. J. Int.,* 117, 653-664.

Özalaybey S., Savage M.K., 1995, Shear-wave splitting beneath western United States in relation to plate tectonics, *J. Geophys. Res.,* 100, 18,135-18,149.

Paczkowski K., Montési L.G.J., Long M.D., Thissen C.J., 2014a, Three-dimensional flow in the subslab mantle, *Geochem. Geophys. Geosyst.,* 15, 3989-4008, doi:10.1002/2014GC005441.

Paczkowski K., Thissen C.J., Long M.D., Montési L.G.J., 2014b, Deflection of mantle flow beneath subducting slabs and the origin of subslab anisotropy, *Geophys. Res. Lett.,* 41, 6734-6742, doi:10.1002/2014GL060914.

Pardo M., Suárez G., 1993, Steep subduction geometry of the Rivera plate beneath the Jalisco block in western Mexico, *Geophys. Res. Lett.,* 20, 2391-2394.

Pardo M., Suárez G., 1995, Shape of the subducted Rivera and Cocos plates in southern Mexico: Seismic and tectonic implications, *J. Geophys. Res.,* 100, 12,357-12,373.

Park J., Levin V., 2002, Seismic anisotropy: Tracing plate dynamics in the mantle, *Science,* 296, 485-489.

Pérez-Campos X., Kim Y., Husker A., Davis P.M., Clayton R.W., Iglesias A., Pacheco J.F., Singh S. K., Manea V.C., Gurnis M., 2008, Horizontal subduction and truncation of the Cocos plate beneath central Mexico, *Geophys. Res. Lett.,* 35, L18303, doi:10.1029/2008GL035127.

Phipps Morgan J., Hasenclever J., Hort M., Rüpke L., Parmentier E.M., 2007, On subducting slab entrainment of buoyant asthenosphere, *Terra Nova,* 19, 167-173, doi:10.1111/j.1365-3121.2007.00737.x.

Polet J., Kanamori H., 2002, Anisotropy beneath California: Shear wave splitting measurements using a dense broadband array, *Geophys. J. Int.,* 149, 313-327.

Ponce-Cortés J.G., 2012, Medición de la anisotropía de las ondas *SKS* en el manto superior, debajo de las estaciones permanentes del Servicio Sismológico Nacional instaladas a partir del año 2005, B. Sc. thesis, 79 pp., Facultad de Ingeniería, Universidad Nacional Autónoma de México, Mexico City, Mexico.

Ramos-Zuñiga L.G., Montalvo-Arrieta J.C., Pérez-Campos X., Valdés-González C., 2012, Seismic characterization of station LNIG as a reference site in northeast Mexico, *Geofís. Int.,* 51, 187-197.

Refayee H.A., Yang B.B., Liu K.H., Gao S.S., 2014, Mantle flow and lithosphere-asthenosphere coupling beneath the southwestern edge of the North American craton: Constraints from shear-wave splitting measurements, *Earth Planet. Sci. Lett.,* 402, 209-220, doi:10.1016/j.epsl.2013.01.031.

Rodríguez-Domínguez M.A., 2016, Transición del ángulo de subducción de la placa de Cocos en la zona centro-sur de México, M. Sc. thesis, 68 pp., Instituto de Geofísica, Universidad Nacional Autónoma de México, Mexico City, Mexico.

Rodríguez-Pérez Q., 2007, Estructura tridimensional de velocidades para el sureste de México, mediante el análisis de trazado de rayos sísmicos de sismos regionales, M. Sc. thesis, 83 pp., Instituto de Geofísica, Universidad Nacional Autónoma de México, Mexico City, Mexico.

Rojo-Garibaldi B., 2011, Anisotropía de las ondas *SKS* en el manto superior debajo de un arreglo sísmico entre Guerrero y Veracruz, B. Sc. thesis, 84 pp., Facultad de Ciencias, Universidad Nacional Autónoma de México, Mexico City, Mexico.

Romo J.M., García-Abdeslem J., Gómez-Treviño E., Esparza F.J., Flores C., 2001, Resultados preliminares de un perfil geofísico a través del desierto de Viscaíno en Baja California Sur, México (in Spanish), *Geos Boletín Informativo de la UGM,* 21, 96-107.

Ruppert S.D., 1992, Tectonics of western North America: A teleseismic view, Ph. D. thesis, 216 pp., Stanford University, Stanford, California, USA.

Russo R.M., Silver P.G., 1994, Trench-parallel flow beneath the Nazca plate from seismic anisotropy, *Science,* 263, 1105-1111.

Satsukawa T., Michibayashi K., Raye U., Anthony E.Y., Pulliam J., Stern R., 2010, Uppermost mantle anisotropy beneath the southern Laurentian margin: Evidence from Knippa peridotite xenoliths, Texas, *Geophys. Res. Lett.,* 37, L20312, doi:10.1029/2010GL044538.

Savage M.K., 1999, Seismic anisotropy and mantle deformation: What have we learned from shear wave splitting?, *Rev. Geophys.,* 37, 65-106.

Savage M.K., Sheehan A.F., 2000, Seismic anisotropy and mantle flow from the Great Basin to the Great Plains, western United States, *J. Geophys. Res.,* 105, 13,715-13,734.

Savage M.K., Silver P.G., 1993, Mantle deformation and tectonics: Constraints from seismic anisotropy in the western United States, *Phys. Earth Planet. Inter.,* 78, 207-227.

Savage M.K., Silver P.G., Meyer R.P., 1990, Observations of teleseismic shear-wave splitting in the Basin and Range from portable and permanent stations, *Geophys. Res. Lett.,* 17, 21-24.

Schellart W.P., 2004, Kinematics of subduction and subduction-induced flow in the upper mantle, *J. Geophys. Res.,* 109, B07401, doi:10.1029/2004JB002970.

Sedlock R.L., 2003, Geology and tectonics of the Baja California peninsula and adjacent areas, in *Tectonic evolution of northwestern Mexico and the southwestern USA, Special Paper 374,* edited by S. E. Johnson, S. R. Paterson, J. M. Fletcher, G. H. Girty, D. L. Kimbrough and A. Martín-Barajas, pp. 1-42, Geological Society of America, Boulder, Colorado, USA, doi:10.1130/0-8137-2347-4.1.

Sedlock R.L., Ortega-Gutiérrez F., Speed R.C., 1993, *Tectonostratigraphic terranes and tectonic evolution of Mexico, Special Paper 278.* Geological Society of America, Boulder, Colorado, USA, 146 pp.

Sheehan A.F., Jones C.H., Savage M.K., Ozalaybey S., Schneider J.M., 1997, Contrasting lithospheric structure between the Colorado Plateau and Great Basin: Initial results from Colorado Plateau-Great Basin PASSCAL experiment, *Geophys. Res. Lett.,* 24, 2609-2612.

Silver P.G., 1996, Seismic anisotropy beneath the continents: Probing the depths of Geology, *Annu. Rev. Earth Planet. Sci.,* 24, 385-432.

Silver P.G., Chan W.W., 1988, Implications for continental structure and evolution from seismic anisotropy, *Nature,* 335, 34-39.

Silver P.G., Chan W.W., 1991, Shear wave splitting and subcontinental mantle deformation, *J. Geophys. Res.,* 96, 16,429-16,454.

Silver P.G., Holt W.E., 2002, The mantle flow field beneath western North America, *Science,* 295, 1054-1057.

Silver P.G., Kaneshima S., 1993, Constraints on mantle anisotropy beneath Precambrian North America from a transportable teleseismic experiment, *Geophys. Res. Lett.,* 20, 1127-1130.

Silver P.G., Savage M.K., 1994, The interpretation of shear-wave splitting parameters in the presence of two anisotropic layers, *Geophys. J. Int.,* 119, 949-963.

Singh S.K., Pacheco J., Courboulex F., Novelo D.A., 1997, Source parameters of the Pinotepa Nacional, Mexico, earthquake of 27 March, 1996 (M_w = 5.4) estimated from near-field recordings of a single station, *J. Seismol.,* 1, 39-45.

Song T.-R.A., Kawakatsu H., 2012, Subduction of oceanic asthenosphere: Evidence from sub-slab seismic anisotropy, *Geophys. Res. Lett.,* 39, L17301, doi:10.1029/2012GL052639.

Stegman D.R., Freeman J., Schellart W.P., Moresi L., May D., 2006, Influence of trench width on subduction hinge retreat rates in 3-D models of slab rollback, *Geochem. Geophys. Geosyst.,* 7, Q03012, doi:10.1029/2005GC001056.

Stein S., Wysession, M., 2003, *An introduction to seismology, earthquakes, and Earth structure.* Blackwell Publishing, Malden, MA, USA, 498 pp.

Stubailo I., 2015, Seismic anisotropy below Mexico and its implications for mantle dynamics, Ph. D. thesis, 119 pp., University of California, Los Angeles, CA, USA.

Stubailo I., Davis P., 2007, Shear wave splitting measurements and interpretation beneath Acapulco-Tampico transect in Mexico, *Eos Trans. AGU,* 88, 52, Fall Meet. Suppl., Abstract T51B-0539.

Stubailo I., Davis P.M., 2012a, Anisotropy of the Mexico subduction zone based on shear-wave splitting analysis (abstract), *Seism. Res. Lett.,* 83, 2, 379.

Stubailo I., Davis P.M., 2012b, Anisotropy of the Mexico subduction zone based on shear-wave splitting and higher modes analysis, Abstract T11A-2538 presented at 2012 Fall Meeting, AGU, San Francisco, CA, 3-7 Dec.

Stubailo I., Davis P.M., 2015, The surface wave, shear wave splitting, and higher mode seismic anisotropy comparison of the Mexican subduction zone (abstract), *Seism. Res. Lett.,* 86, 2B, 677.

Stubailo I., Beghein C., Davis P.M., 2012, Structure and anisotropy of the Mexico subduction zone based on Rayleigh-wave analysis and implications for the geometry of the Trans-Mexican Volcanic Belt, *J. Geophys. Res.,* 117, B05303, doi:10.1029/2011JB008631.

Suarez G., Singh S.K., 1986, Tectonic interpretation of the Trans-Mexican Volcanic Belt — Discussion, *Tectonophysics,* 127, 155-158.

Trampert J., Paulssen H., van Wettum A., Ritsema J., Clayton R., Castro R., Rebollar C., Pérez-Vertti A., 2003, New array monitors seismic activity near the Gulf of California in Mexico, *Eos Trans. AGU,* 84, 29, 32.

Valdés-González C., Cárdenas-Ramírez A., Cruz-Cervantes J.L., Estrada-Castillo J., Pérez-Santana J., Santiago-Santiago J. A., Jiménez-Cruz C., Gutiérrez-García A., Rubí-Zavala B., 2005, ¿20 años después del sismo de 1985, sísmicamente qué le falta a la red del Servicio Sismológico Nacional? (abstract), *Geos Boletín Informativo de la UGM,* 25, 1, 185.

Valdés-González C., Jiménez-Cruz C., Espíndola-Castro V.H., Estrada-Castillo J.A., Pérez-Santana J.A., Franco-Sánchez S. ., Cárdenas-Monroy C., Li-Tan Y., Cárdenas-Ramírez A. B., Cruz-Cervantes J.L., Navarro-Estrada F., Rodríguez-Rasilla I., Hurtado-Díaz A., Arreola-Manzano J., Caballero-Jiménez G.V., González-López A., Hernández-Valdivia L., Vidal-Amaro M., 2012, El Servicio Sismológico Nacional: Actividad sísmica 2011-2012 en México (abstract), *Geos Boletín Informativo de la UGM,* 32, 1, 262.

Valenzuela-Wong R., León-Soto G., van Benthem S., Bernal-Díaz A., Bernal-López L., Ponce-Cortés G., Rojo-Garibaldi B., 2015, Anisotropía sísmica y flujo del manto superior en la zona de subducción de las placas de Cocos y Rivera en México, Abstract SR02-2 presented at the 2015 Meeting "Avances y retos en Sismología, Ingeniería y Gestión de riesgos a 30 años del sismo de 1985", Mexico City, Mexico, 17-19 Sept.

Van Benthem S.A.C., 2005, Anisotropy and flow in the uppermantle under Mexico, M. Sc. thesis, 41 pp., Utrecht University, Utrecht, The Netherlands.

Van Benthem S.A., Valenzuela R.W., 2007, Upper mantle shear wave anisotropy for stations in Mexico and its relationship to subduction at the Middle America Trench, *Eos Trans. AGU,* 88, 23, Jt. Assem. Suppl., Abstract S51C-07.

Van Benthem S.A.C., Valenzuela R.W., Obrebski M., Castro R.R., 2008, Measurements of upper mantle shear wave anisotropy from stations around the southern Gulf of California, *Geofís. Int.,* 47, 127-143.

Van Benthem S.A.C., Valenzuela R.W., Ponce G.J., 2013, Measurements of shear wave anisotropy from a permanent network in southern Mexico, *Geofís. Int.,* 52, 385–402, doi:10.1016/S0016-7169(13)71485-5.

Vauchez A., Nicolas A., 1991, Mountain building: Strike-parallel motion and mantle anisotropy, *Tectonophysics,* 185, 183-201.

VEOX, 2010, Veracruz-Oaxaca subduction experiment, Caltech, dataset, Pasadena, CA, USA, doi:10.7909/C3MW2F2C.

Vinnik L.P., Kind R., 1993, Ellipticity of teleseismic *S*-particle motion, *Geophys. J. Int.,* 113, 165-174.

Vinnik L.P., Kind R., Kosarev G.L., Makeyeva L. I., 1989a, Azimuthal anisotropy in the lithosphere from observations of long-period *S*-waves, *Geophys. J. Int.,* 99, 549-559.

Vinnik L.P., Farra V., Romanowicz B., 1989b, Azimuthal anisotropy in the Earth from observations of *SKS* at Geoscope and NARS broadband stations, *Bull. Seism. Soc. Am.,* 79, 1542-1558.

Vinnik L.P., Makeyeva L.I., Milev A., Usenko A. Yu., 1992, Global patterns of azimuthal anisotropy and deformations in the continental mantle, *Geophys. J. Int.,* 111, 433-447.

Vinnik L., Romanowicz B., Le Stunff Y., Makeyeva L., 1995, Seismic anisotropy in the D" layer, *Geophys. Res. Lett.,* 22, 1657-1660.

Vinnik L.P., Green R.W.E., Nicolaysen L. O., 1996, Seismic constraints on dynamics of the mantle of the Kaapvaal craton, *Phys. Earth Planet. Inter.,* 95, 139-151.

Wang Y., Forsyth D.W., Savage B., 2009, Convective upwelling in the mantle beneath the Gulf of California, *Nature,* 462, 499-502.

Wessel P., Smith W.H.F., 1998, New, improved version of Generic Mapping Tools released, *Eos Trans. AGU,* 79, 579.

Wiens D.A., Conder J.A., Faul U.H., 2008, The seismic structure and dynamics of the mantle wedge, *Annu. Rev. Earth Planet. Sci.,* 36, 421-455, doi:10.1146/annurev.earth.33.092203.122633.

Wolfe C.J., Silver P.G., 1998, Seismic anisotropy of oceanic upper mantle: Shear wave splitting methodologies and observations, *J. Geophys. Res.,* 103, 749-771.

Wookey J., Kendall J.M., 2004, Evidence of midmantle anisotropy from shear wave splitting and the influence of shear-coupled *P* waves, *J. Geophys. Res.,* 109, B07309, doi:10.1029/2003JB002871.

Wookey J., Kendall J.M., Barruol G., 2002, Mid-mantle deformation inferred from seismic anisotropy, *Nature,* 415, 777–780.

Wüstefeld A., Bokelmann G., Barruol G., Montagner J.P., 2009, Identifying global seismic anisotropy patterns by correlating shear-wave splitting and surface-wave data, *Phys. Earth Planet. Inter.,* 176, 198-212, doi:10.1016/j.pepi.2009.05.006.

Yang T., Grand S.P., Wilson D., Guzmán-Speziale M., Gómez-González J.M., Domínguez-Reyes T., Ni J., 2009, Seismic structure beneath the Rivera subduction zone from finite-frequency seismic tomography, *J. Geophys. Res.,* 114, B01302, doi:10.1029/2008JB005830.

Zhang S., Karato S.-I., 1995, Lattice preferred orientation of olivine aggregates deformed in simple shear, *Nature,* 375, 774–777.

Zhang X., Paulssen H., Lebedev S, Meier T., 2007, Surface wave tomography of the Gulf of California, *Geophys. Res. Lett.,* 34, L15305, doi:10.1029/2007GL030631.

Zhang X., Paulssen H., Lebedev S, Meier T., 2009, 3D shear velocity structure beneath the Gulf of California from Rayleigh wave dispersion, *Earth Planet. Sci. Lett.,* 279, 255-262, doi:10.1016/j.epsl.2009.01.003.